Article:

Inkjet printing of mammalian cells – Theory and applications

Piyush Kumar [a], Stephen Ebbens [a], Xiubo Zhao [a,b,*]

[a] *Department of Chemical and Biological Engineering, University of Sheffield, Sheffield, S13JD, UK*
[b] *School of Pharmacy, Changzhou University, Changzhou, 213164, China*

A B S T R A C T

Inkjet bioprinting is a new and versatile technology which has found novel applications in cell biology and associated biomedical research. Cells suspended in a low-viscosity liquid medium can be readily dispensed using piezoelectric and thermal actuation-based drop-on-demand inkjet printers, which are the most commonly used inkjet printing technologies. As inkjet printing has the advantage of producing high resolution and high precision prints, it is one of the most suitable technologies for bottom-up cell deposition for building intricate biological constructs. In addition, with the use of appropriate bioinks, inkjet printing can produce both, 2D as well as 3D structures. This review paper is an attempt to curate inkjet bioprinting research, with an exclusive focus on mammalian cells, and comprehend the main application areas, such as intracellular delivery and transfection, gene expression modification, single cell sorting, cell microarray, cell micropatterning, tissue engineering, and *in vivo* cell printing. The printability of cells has also been discussed in order to understand how the process of inkjet bioprinting affects the cellular mechanics and physiology and subsequent survival, proliferation and differentiation.

1. Introduction

Inkjet printing is a 'bottom-up' approach to fabricating structures as opposed to the conventional 'top-down' approach. Inkjet printing is also known as droplet based printing because the ink is jetted through the nozzle of a jetting device in the form of droplets with nano-to pico-litre volume range [1,2]. The deposition pattern or the design of the structure to be printed is pre-defined using a computer-aided design (CAD) software [2,3]. A computer comprehends the 2D or 3D design and accordingly sends electrical signals to move either the stage which holds the substrate, or the printhead which holds the jetting device, as the ink is ejected and deposited on the substrate.

1.1. Types of inkjet printing

On the basis of the actuation technique or the mode of jetting, inkjet printing can be classified into two main variants, namely, thermal and piezoelectric [1,3,4], as illustrated in Fig. 1. In thermal inkjet printing, a heating device surrounds the jetting device which holds the fluid ink. When the CAD signal is received from a computer, the heating device quickly heats up, causing a sudden expansion of fluid volume resulting in the jetting [1,3,4]. In piezoelectric inkjet printing, on the other hand,

a piezoelectric material surrounds the fluid cavity of the jetting device. Piezoelectric materials are certain solid materials which undergo mechanical deformations in response to an applied electric field and vice versa [3,4]. As a result, when the CAD signal is received, the piezoelectric material contracts in a pre-defined manner and causes ejection of the fluid out of the nozzle [2–4]. Other actuation techniques are electrostatic, electrohydrodynamic, solenoid-valve and acoustic inkjet printing [5]. These, however, are much less commonly used owing to their major limitations, which are, the necessity to have a conductive ink in the case of electrostatic and electrohydrodynamic inkjet printing; large droplet sizes at 500 μm or more causing low resolution printing in the case of solenoid-valve inkjet printing; and the necessity for upside down substrate placement in case of acoustic printing [5–7].

On the basis of the mode of deposition of the ink, inkjet printing can be either continuous or drop-on-demand [1,8,9]. In continuous inkjet (CIJ) printing, a conductive fluid ink is jetted very fast, almost in the form of a continuous stream. After jetting, the ink is electrically charged and passed through an electrical field, which deflects the ink droplets towards the substrate in accordance to the CAD signal received from the computer. The non-deflected droplets are recycled and sent to the reservoir in the printhead so that they can be used for printing again [1, 8,9]. In drop-on-demand (DOD) inkjet printing, the jetting device

---

* Corresponding author. Department of Chemical and Biological Engineering, University of Sheffield, Sheffield, S1 3JD, UK.
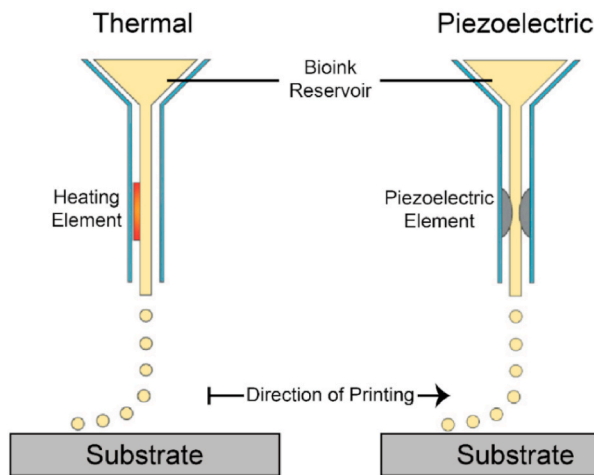*E-mail address:* xiubo.zhao@sheffield.ac.uk (X. Zhao).

Fig. 1. Schematic illustration of thermal and piezoelectric inkjet printing processes. [image adapted from Ref. [10] Copyright © 2016 IOP Publishing Ltd].

actuates and jets out the ink droplets only when the signal is received on the basis of the CAD. For the correct placement of the deposited ink material, either the printhead or the substrate moves in X-Y-Z Cartesian coordinates [1,8,9].

1.2. Inkjet bioprinting

Inkjet printing technologies are used in a wide range of sectors, such as, electronics [11–13], tissue engineering [2,9,14], and therapeutics research [15,16]. When inkjet printing is applied in biomedical research, such as tissue engineering, it is referred to as inkjet bioprinting and the materials (or biomaterials) which are printed are called bioinks if formulated with cells, or biomaterial inks if formulated without cells [17,18]. Of the two, DOD inkjet printing is used for biomedical applications rather than CIJ as the recirculation of bioink in the latter can potentially cause contamination [9]. The use of inkjet printing technology for printing cells was reported first in 2003 by Boland et al. [19–21]. The researchers modified a commercial paper printer and its cartridges based on thermal inkjet technology and successfully printed mammalian cells (bovine aortal endothelial cells and smooth muscle cells) suspended in cell culture medium. The cell printing was conducted initially as a 2D straight line [20], and then as several layers on top of each other, alternating with layers of a thermosensitive gel, to form a 3D straight line on a substrate [21]. Inkjet bioprinting can effectively and precisely deliver cells in high throughput and thus act as a precursor for propagating research on various biomedical applications, such as development of advanced lab-on-a-chip devices, which require precise localization of cells at millimetre to micron scale [22–24]. As the depositing droplets can be as small in volume as being in the picolitre range, inkjet bioprinting offers very high printing resolution and precise cell placement [25]. Because of its higher printing resolution and smaller printing footprint, inkjet printing is more suitable for direct cell printing in comparison to other available printing technologies, such as, extrusion printing, laser induced forward transfer and stereolithography. It is also easily scalable, potentially to industrial scale, as several printheads, each with multiple nozzles, can perform printing together [1,26]. Inkjet bioprinting is, therefore, also an environmentally friendly technology as it uses much less amounts of raw materials, such as cells and suspension media, and produces much less biological wastes. Thus, it is understandable that inkjet bioprinting is lesser resource-intensive, faster and more cost effective [27] and, therefore, more favourable in conducting biomedical research involving the printing of mammalian cells for such applications as single cell sorting [28], cell microarray [29] and cell micropatterning [30]. Inkjet

bioprinting also offers a non-contact strategy [1,31] for cell deposition which has several advantages over other methods, such as, micro-contact printing [32–35] and micro-well trapping [36–38], which require direct contact with the cells. Some of these advantages are – a much lesser risk of cross-contamination among the post-printed/immobilized cells, ability to deposit cells on variety of substrates [1,4,14] and a much higher flexibility in cell size variation and deposition patterns and spacing [28].

1.3. Scope of this review

This paper explores, compiles and reviews the past and the present of mammalian cell printing using the inkjet bioprinting technology. Majority of research on inkjet bioprinting of mammalian cells is done with such bioinks in which the cells are suspended in a printable liquid scaffold-precursor, such as fibrinogen, which usually requires in-printing or post-printing curing, that is, cross-linking or polymerization, to obtain the final cell-laden structure in the required layout or shape. Such research is primarily devoted to 3D cell micropatterning, 3D organoid modelling, tissue engineering and *in vivo* cell printing. The other, relatively less researched approach, is printing mammalian cells suspended in a scaffold-precursor-free liquid medium, such as cell culture medium, on a variety of substrates for faster and accurate yielding of 2D cellular patterns. Such research is primarily devoted to building high-throughput lab-on-a-chip devices for conducting various biomedical assays aimed at disease modelling, drug screening, toxicology tests, immunocytochemistry and other single cell analyses [3,39]. Our review is structured to first of all discuss the viability of cells following printing in light of the mechanical and thermal stresses associated with this process. Then we discuss how the temporary formation of pores caused by the deformations associated with printing in fact provides a route to intracellular delivery of molecular and genetic material, giving opportunities for new research methods. Equally important, we summarize research on the gene expression changes that are associated with printing, which are vital to screen for printed cells having unexpected modified behaviours which could hamper their uses, or alternatively provide opportunities to be exploited. The second part of the review then considers the challenges associated with using inkjet bioprinting to generate increasingly complex structures, with a range of potential applications. This section starts by describing cell-sorting, in this context to enable on demand deposition of a well-controlled number of cells, down to individuals. Cell-sorting is an enabler for the subsequently described patterning methods, ranging from cell microarrays which can assist screening, to cell micropatterns with applications in lab-on-a-chip devices, and tissue cultures which can mimic entire complex biological structures. While these entities are all made outside the body, we finally describe the potential for printing to be performed directly *in vivo*, for example to promote wound healing. In addition, a table has been included (Table 1) to summarize the areas of application with comparison of thermal and piezoelectric inject printing and their pros and cons.

2. Printability of cells

With the inception of inkjet printing of cells and continuous evolution in the inkjet bioprinting technology, it became essential to know how the direct jetting process affects cellular mechanics, metabolism and physiology through thermal stress and mechanical stress, such as shear, tension, and compression.

2.1. Computational modelling analysis

Research has been conducted to simulate cell printing and developed mathematical models to judge the extent of printability of cells. Sohrabi et al. [68] used the modified pseudopotential model and thermal model of lattice Boltzmann method (LBM) for modelling and simulating the thermal inkjet cell printing process. The LBM is a mesoscopic CFD

Table 1

List of areas of application discussed in this review and a brief comparison between the thermal and piezoelectric inkjet printing techniques with respect to their benefits and limitations in each area of application.

Applications	Inkjet Technique with Benefits/Limitations	Ref.
Intracellular delivery and transfection	Thermal technique results in pore formation by both heat shock and shear stress but with lesser controllability on pore size. Piezoelectric technique causes pore formation by shear stress and provides the ability to control pore size by changing voltage.	[40–42] [22]
Gene expression modification	Changes in gene expression occur, but currently it is not possible to selectively and precisely manipulate and control the expression level of a particular gene. Thermal technique also causes heat shock response in cells alongside changes in gene expression. Therefore, piezoelectric technique is a relatively safer method.	[43–45] [46]
Single cell sorting	More research is available with piezoelectric technique than with thermal technique. Overall well-researched but requires sophisticated camera and tracking software setup to ensure only one cell per droplet.	[47] [28, 48–51]
Cell microarray	Both thermal and piezoelectric techniques have shown promising results for single and fixed number of multiple cell deposition for conducting cell-based assays.	[29, 52–54]
Cell micropatterning	Both thermal and piezoelectric techniques provide excellent ability of high precision 2D and 3D cell micropatterning to imitate tissue architecture *in vitro*.	[30, 55–59]
Tissue engineering	Very promising and higher precision but limited by small volumetric output causing slower than required speed. Some research has focussed on combining inkjet with other printing techniques, such as spray printing and extrusion printing.	[60–63] [27,64]
in vivo cell printing	Good alternative to graft implants. But still a largely theoretical area of application. Much more research is required. Holds potential if integrated with robotics and automation technologies.	[65,66] [67]

(computational fluid dynamics) method for the numerical simulation, investigation and understanding of complex fluid flow systems, including, but not limited to, thermal flows, turbulent flows and multiphase flows [69,70]. The authors base the modelling and simulation of the cell bioprinting process on the geometrical configuration of an HP60 inkjet cartridge with a narrow nozzle channel of 48 μm in diameter. The heating resistors in the cartridge heat for 3 μs, causing an explosive formation of vapour bubble, whose pressure reaches up to 8–12 MPa. This cartridge ejects droplets with a velocity of 12 m/s. For the simulation, the authors assumed a simplified cellular structure in accordance to the spring network model, which has been widely used to simulate cells [71–73], as the mechanics of a real cell are extremely complex. In the spring network model, the cell membrane and nuclear membrane are considered to constitute a set of vertex nodes connected together by springs forming a 2D triangulated network, whereas the cytoplasmic actin fibres are considered as linear springs [74,75]. The diameter of the resultant modelled cell is taken as 16 μm. Cell damage during thermal inkjet bioprinting can happen by thermal shock and by mechanical deformations. It is, however, found that the heat shock is critical only in the vicinity of the heating element and most cells, therefore, remain insulated and unaffected while floating in the surrounding liquid medium. The force from the thermal shock and the heightened fluid pressure at the nozzle of the jetting device cause a temporary deformation in the cells during ejection. Fig. 2 (a) shows a simulation of time sequence of cellular deformation as a 16 μm cell

(grey) gets jetted out of a 48 μm nozzle along with the surrounding liquid medium droplet (red) during inkjet bioprinting. At smaller scale, cellular deformation also manifests as the formation of several nanopores, thus, releasing most of the membrane deformation energy and preventing the cells from rupturing. Similar results were found in the work by Koshiyama and Wada [76], who analysed the effects of mechanical stress on a 2D phospholipid bilayer, which is similar to a cell membrane. They performed numerical simulations on the pore formation dynamics arising from equibiaxial (equal in both X and Y axes) stretching applied on a computationally modelled 2D phospholipid bilayer. The results showed an anisotropic deformation of the bilayer membrane and an ingress of water in the hydrophilic regions of the bilayer through the formed pores, which eventually leads to rupturing of the bilayer only if a pore's critical area is exceeded. The results also showed that a higher stretching speed increases the statistical probability of formation of several small pores and increases the required apparent bilayer breaking force from 250 pN in quasistatic stretching to 300, 350 and 450 pN in unsteady stretching with the stretching speeds of 0.1, 0.3 and 1.0 m/s, respectively. This increase in the apparent breaking force with an increase in the stretching speed indicates viscoelastic nature of the bilayer.

2.2. Live cell analysis: Non-human mammalian cells

Furthermore, in order to determine whether the positive results from computational modelling and simulation also hold true in real applications, several experiments have been conducted to prove that inkjet printing of mammalian cells is a very feasible technique. The commercially available inkjet paper printers are usually based on thermal inkjet printing technology. Researchers have been able to modify such commercial printers and their ink cartridges for the deposition of mammalian cells, such as, Chinese hamster ovary (CHO) cells suspended in Dulbecco's phosphate buffered saline (DPBS) solution [42,55] in pre-defined patterns with different printing settings, such as voltage, pulse width and frequency. In these studies, the post-printing analyses of the CHO cells showed less than 8–10% of cells undergoing lysis in one case [55], and an 89% cell viability with only 3.5% of apoptotic cells in another case [42], indicating an insignificant amount of cell lysis during printing. In early research by Nakamura et al. [24], post-printing culture of bovine vascular endothelial cells and its comparison with the control non-printed cells revealed no morphological variations and structural damages even under the high magnification of scanning electron microscopy. Live imaging of the inkjet nozzle, where maximum shear stress occurs, during the printing of adult rat retinal cells and glial cells suspended in culture medium, has confirmed that no significant distortion or cellular destruction occurs during the jetting process, as shown in Fig. 2 (b – c) [77]. In another proof of concept study, Detsch et al. [78] printed ST-2 clonal stromal cell line, derived from the bone marrow of BC8 mice and suspended in thrombin solution, on a fibrinogen film substrate using a piezoelectric inkjet printer. No adverse effects on the cells were observed by a fluorescence cell viability assay after 24 h of incubation post-printing. One major area of study in bioprinting is the controlled and reproducible deposition of neurons for developing increasingly complex neuronal networks and functional *in vitro* brain-like models for performing research on and understanding various brain pathologies and neural diseases [25,79,80]. In one such study, Xu et al. [56] have printed rat primary embryonic hippocampal and cortical neurons, suspended in DPBS solution, in 2D circular patterns using a modified commercial thermal inkjet printer. The viability and electrophysiology of the cells were analysed post-printing. Within a day after printing, the cells started showing differentiation and development of processes. A cell viability of 74.2 ± 6.3% was obtained on day 8 post-printing. Positive immunostaining with neuronal-specific markers confirmed that the printed neurons were able to maintain their normal and healthy cellular physiology and functions. Whole-cell patch-clamp recording was performed after 2 weeks of culture to evaluate the
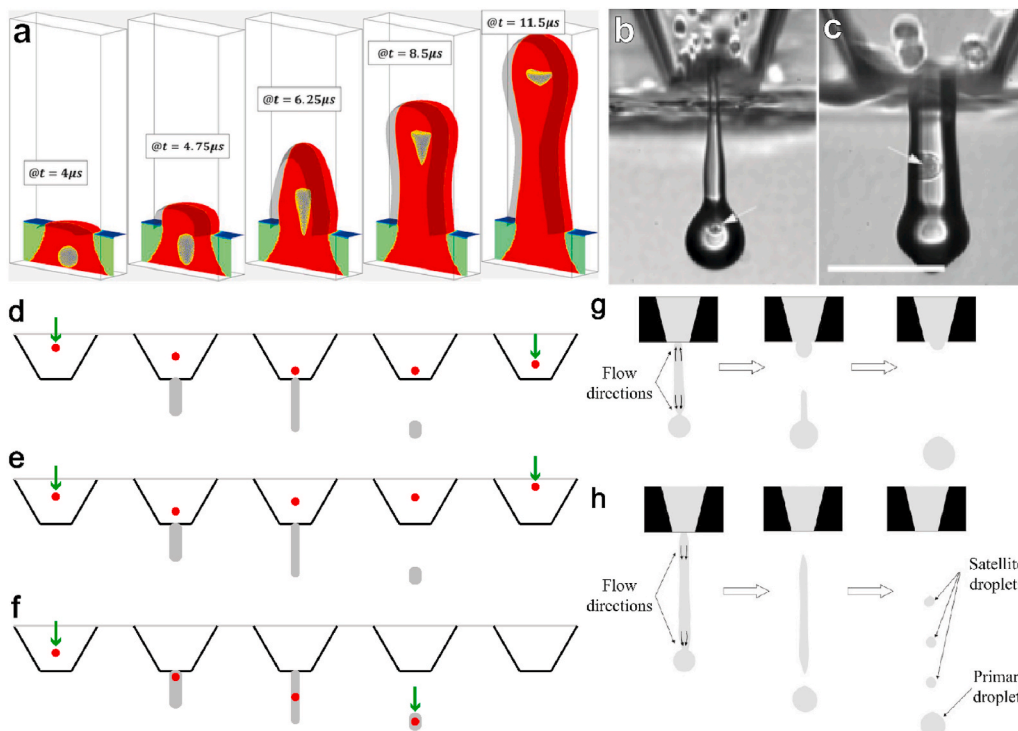
Fig. 2. (a) Time sequence illustration of simulation of cell deformation as the cell (grey) squeezes, along with the surrounding liquid medium (red), through the nozzle of the jetting device of an inkjet printer. Maximum cellular deformation is observed at t = 6.25 μs, after which the cell readily returns back to its original shape. [image (a) republished with permission from Ref. [68] Copyright © 2018 American Physical Society]. Close up images of the nozzle of a jetting device showing **(b)** a retinal cell and **(c)** a glial cell (indicated by white arrows) inside a droplet just after jetting. It is clearly observable that the cells are able to maintain their native spherical shape without any deformation or rupture after getting jetted out (scale bar: 100 μm). [images (b–c) republished with permission from Ref. [77] Copyright © 2014 IOP Publishing Ltd]. **(d–f)** Cells' vertical motion behaviour during droplet ejection in inkjet printing depends on the rheological properties of the surrounding liquid medium, illustrated here as simplified time sequences (red = cells, grey = droplets, green arrows = cell positions); **(d)** cell travel occurs when the final position of a cell is nearer to the orifice than its initial position; **(e)** cell reflection occurs when the final position of a cell is farther from the orifice than its initial position; **(f)** cell ejection occurs when a cell exits the nozzle along with the ejected droplet. **(g–h)** Schematic illustration of two types of droplet ligament formation and ligament flow during jetting depending on the voltage of the piezoelectric actuation; **(g)** 30 V; **(h)** 60 V [images (g–h) adapted from Ref. [83] Copyright © 2017 AIP Publishing]. (For interpretation of the references to color in this figure legend, the reader is referred to the Web version of this article.)

development of voltage-gated ion channels. The measurements of outward K^+ and inward Na^+ currents showed that the printed and cultured cells had developed into mature neurons. In another similar research [55], rat primary embryonic motor neurons were suspended in DPBS solution and printed using a modified commercial HP550C printer and its modified HP51626a ink cartridge. The cells were deposited in specific patterns on biologically derived substrates, such as soy agar and collagen gel, which help in cell survival and growth during the post-printing culture. Not only the motor neurons show a >90% post-printing viability, they also begin developing processes, or axon and dendrites, and establishing polarized morphologies by the 2nd day after printing.

2.3. Live cell analysis: Human cells

Such promising results during initial research on inkjet bioprinting of animal, particularly mammalian, cells have paved the way for similar studies with human cells. In a research [78], the HCT116 human colorectal carcinoma cells, suspended in RPMI medium with 10% foetal calf serum, were printed using a piezoelectric inkjet printer. The authors tested 32 different printing settings across 3 different parameters to study their effects on the cells. The three parameters were voltage (20–150 V), voltage pulse time or width (20–200 μs) and frequency of droplets (50–1000 Hz). The cell viability assay 48 h post-printing showed that the most viable cell sample is the one printed at 100 V with 100–150 μs pulse width while being independent of any effect from the frequency. This shows that an appropriate voltage and pulse width, which leads to a proper droplet formation, also in turn results in the maximum achievable cell viability. Interestingly, in another study with human cells (alongside other mammalian cells), no significant correlation could be found between the printing voltage and post-printing cell

viability. In this study, Tse et al. [23] used a piezoelectric inkjet printer to print human dermal fibroblast cells, porcine Schwann cells and the rat neuronal analogue NG108-15 cells. A jetting device with nozzle diameter of 60 μm was used and a voltage range of 70–230 V was applied for printing. The cell viabilities were >90% for all control samples, 82–92% for human fibroblasts, 89–92% for porcine Schwann cells and 86–96% for rat NG108-15 cells, as measured for up to 7 days post-printing. In a similar study, Saunders et al. [81] studied the effects of mechanical stress on the HT1080 human fibroblast cells suspended in DMEM and printed at a very high frequency of 10 kHz, a pulse width of 20 μs and a voltage range of 30–80 V with a piezoelectric actuated drop-on-demand inkjet bioprinter. The cells were printed directly on a well plate surface and kept in incubation after the addition of culture medium. Live/dead cell viability assay revealed a >90% cell survival rate as measured up to 96 h post-printing under all printing conditions.

2.4. Cell behaviour analysis

It is, therefore, safe to assume that a very high post-inkjet-printing cell viability is readily achievable, even though there may occur minor variations among different batches and among different research groups depending on the cell type, the type of nozzle and printer, the printing parameters, and the post-printing culture conditions. Another important aspect, however, is to understand how the cell behaviour during ejection is affected by the fluid dynamics inside the nozzle of the jetting device. This ultimately affects the printing efficiency and the post-printing cell viability. To track and analyse the cell motion during actuation and ejection, Cheng et al. [82] used piezoelectric nozzles, measuring 21.7 mm in length and 80 μm in orifice diameter, to print MCF-7 human breast cancer cells, with an average diameter of 15 μm, suspended in PBS solution. Cell positions were ascertained by stained cell tracking using

high speed imaging with low depth of field and subsequent image processing using an algorithm in MATLAB. With each ejected droplet, three types of cell behaviour were observed on the basis of cells' net vertical motion, classified and termed by the authors as cell travel, cell reflection, and cell ejection, as illustrated in Fig. 2 (d – f). Cell travel was defined as the net displacement of a cell towards the nozzle orifice at a droplet ejection event and then stabilising at a position within the nozzle nearer to the orifice than initial position. Cell reflection was the opposite of cell travel and defined as the net displacement of a cell away from the orifice and towards the cell reservoir at a droplet ejection event. Initially, the cell did move towards the orifice along with the fluid flow, but then got projected away as the droplet broke off, stabilising at a position within the nozzle farther from the orifice than initial position as the meniscus oscillated and dampened gradually. Cell ejection occurred when a cell exited the nozzle along with the ejected droplet. On mixing a higher density and viscosity medium, Ficoll PM400 at 10% (w/v) in PBS, the cell reflection behaviour was eliminated. While printing the PBS cell suspension with 1.07 mPa s viscosity, the positions of 134 cells were mapped, of which, 78, 37 and 18 cells experienced cell travel, cell ejection and cell reflection, respectively. In Ficoll PM400 cell suspension with 4.86 mPa s viscosity, of the 138 mapped cells, 102 and 36 experienced cell travel and cell ejection, respectively, while no cell reflection was observed. A more viscous Ficoll PM400 solution made the medium neutrally buoyant to the cells, thus preventing both, cell sedimentation near the nozzle orifice, and cell reflection. The authors, thus, demonstrated the importance of liquid medium and its rheological properties in influencing the observed cell behaviour and determining the outcome and efficiency of inkjet cell printing. In a similar research, Zhang et al. [83] have analysed the geometry and behaviour of the cell-laden droplets during and after ejection and their effects on post-printing cell viability and cell distribution. 3T3 mouse fibroblasts, suspended in 1% (w/v) alginate solution in DMEM, were ejected using a commercial piezoelectric inkjet printer and a jetting device with 120 μm orifice diameter. The cell-laden alginate droplets were deposited into calcium chloride solution, which cross-linked alginate, forming cell-containing alginate microspheres. The spheroids were assessed for cell density and cell viability and from the results, the authors derived three conclusions. First, at a lower actuation voltage of 30 V, the droplet ligament moved in two opposite directions, one upwards back into the nozzle, and one downwards breaking off and becoming the final ejected droplet as shown in Fig. 2 (g). At a higher voltage of 60 V, the ligament flow remained unidirectional and downwards, breaking off at the orifice into one large primary droplet and several small satellite droplets as shown in Fig. 2 (h). The different flow directions were a result of the competition between the ejection pressure pulse and the capillary pressure. Second, as discernible, fewer cells were printed at the lower voltage than at the higher voltage. In the 30 V printed samples, 44% of the microspheres contained no cells and the microspheres containing 1, 2 and 3 or more cells were 28%, 19% and 9%, respectively. In contrast, in the 60 V printed samples, only 9% of the microspheres contained no cells and the microspheres containing 1, 2, and 3 cells were 21%, 23% and 47%, respectively. Third, the viability of the cells printed through both the types of ligament flow was same at around 90% without any significant difference, as measured at different time points for up to 2 days post-printing.

Success of such research as elaborated in this section in assuring very high post-printing cell viability and normal cellular physiology, growth and differentiation after inkjet bioprinting and detailed assessment of printing controllability has paved the way for more focussed and complex research with mammalian and human cell printing.

3. Intracellular delivery and transfection

Conventionally, intracellular delivery or transfection is conducted mostly through electroporation in which the cells are mixed with the molecules or genes to be delivered or transfected and then exposed to electrical pulses, which temporarily disrupts the cell membrane leading to an increase in its permeability [84,85]. Other gene transfection techniques involve the use of viral vectors [86,87] and non-viral vectors, such as liposomes [88–90] which are engineered to carry the desired molecules or genes. Electroporation and the other techniques, however, have severe limitations including cytotoxicity, use of expensive reagents, and low delivery or transfection rates, especially with primary cells, stem cells and non-dividing resting cells [42,91]. The electroporation-based proprietary nucleofection technique helps resolve some of these issues, but the post-nucleofection cell viability is relatively lower (11–75%) [40,91–93] in comparison to the post-inkjet-printed cells (74–96%) [23,40,42,55,56,81]. As mentioned in the previous section, the thermal and mechanical stresses acting on the simulated cells during the inkjet printing process has been found to cause the formation of nanopores on the cell membrane [68]. This causes a temporary increase in the cell membrane permeability, and as the cells do not rupture if the nanopores are below a critical limit in size, this phenomenon is being explored as a potential route for intracellular delivery of biologically active molecules and transfection of genes [31].

3.1. Thermal inkjet printing based research

In one of the first such studies [40], Xu et al. transfected plasmids encoding the green fluorescent protein (GFP) into the porcine aortic endothelial (PAE) cells, suspended in the proprietary nucleofection buffer, using a modified commercial thermal inkjet printer and its cartridge (jetting device), as illustrated in Fig. 3 (a). The successfully transfected cells expressed GFP strongly over the 10-day observation period. On comparing with other transfection techniques, the transfection rate of inkjet printing (12.8%) was found to be higher than that of the liposome-based transfection (10.6%), but lower than that of the electroporation-based transfection (32.3%). However, the post-transfection viability of these cells was as high as 90%. In comparison, the cell viability in electroporation and lipofection methodologies was found to be much lower between 40 and 60% across different repeats and replicates. The researchers also analysed the effects of nozzle diameter of the jetting device and plasmid size on the transfection efficiency. The jetting device with narrower nozzle (HP 51629a), which caused higher shear stress, resulted in higher transfection rate (14.1%) in comparison to the jetting device with wider nozzle (HP 51626a) (4.1%). The smaller pmaxGFP plasmid (3.2 kb) resulted in a much higher transfection rate (14.1%) than the larger pIRES-VEGF-GFP plasmid (6.3 kb) (1.1%). Additionally, agarose gel electrophoresis of solo printed GFP plasmids showed normal plasmid content without any evident structural damage and background DNA smearing, similar to the control sample. In a similar research [42], CHO cells mixed with GFP plasmids were suspended in DPBS solution and printed to evaluate the gene transfection potential of inkjet printing methodology. On fluorescence imaging, GFP was found to be expressed in around 30% of the post-printed cells, indicating a relatively higher transfection efficiency than in the previous research. Afterwards, the researchers analysed and comprehensively evaluated the nanopores that developed on the membrane of CHO cells, suspended in DPBS solution, after thermal inkjet printing. The printed CHO cells were stained with propidium iodide and Texas Red conjugated dextran molecules of different molecular weights (MW), all of which are impenetrable through a healthy cell membrane. On fluorescence imaging, 70k MW dextran, with Stokes diameter (SD) of 120 Å, could not be found inside the cells, indicating that the pore size is less than 120 Å or 12 nm. Dextran with molecular weights of 40k (SD = 90 Å), 10k (SD = 46 Å) and 3k (SD = 28 Å) and propidium iodide (SD = 16 Å) were all detectable inside the cells. However, on staining the cells at different time intervals post-printing, it was found that 40k dextran, 10k dextran, 3k dextran and propidium iodide were detectable inside the cells for only up to 0.25, 0.25, 1 and 1.5 h, respectively, after printing. No staining molecule was detectable on staining the cells at 2 h post-printing. This indicates the transient nature of the nanopores and
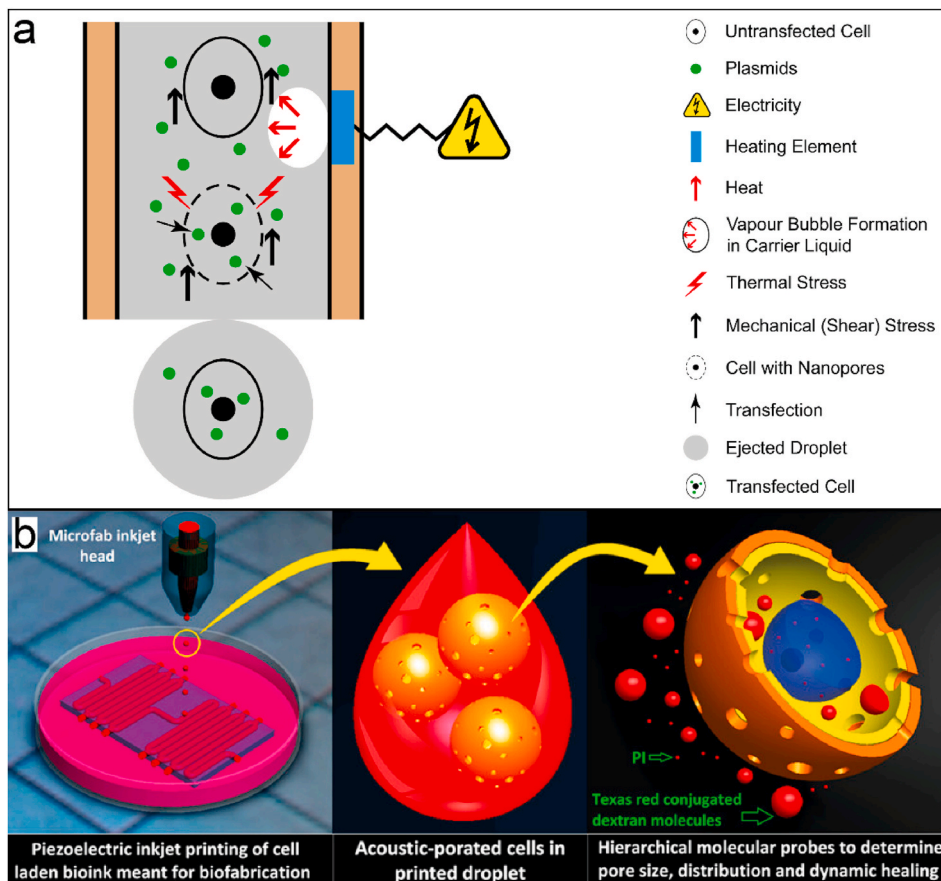
Fig. 3. (a) Schematic illustration of longitudinal section of the jetting device of a thermal inkjet printer printing cells mixed with plasmids. The thermal and mechanical stresses cause a temporary and limited disruption in the cell membrane. This causes an enhanced cellular permeability leading to gene transfection. **(b)** Schematic illustration of piezoelectric inkjet printing of cells and the resulting formation of transient nanopores on the cell membrane due to mechanical stress. Subsequently, intracellular delivery of molecules, such as dextran, is easily achieved through these nanopores. [image (b) republished with permission from Ref. [22] Copyright © 2019 American Chemical Society].

the cell membrane returning back to its normal and healthy state. Owczarczak et al. [41] have also comprehensively examined the size and the transient nature of the nanopores on the 3T3 mouse fibroblasts suspended with fluorescently labelled g-actin monomers in PBS solution and jetted using a modified commercial thermal inkjet printer. The printing process created nanopores of around 10 nm in diameter on the cell membrane without affecting cell viability, as shown in the post-printing cell culture and analysis results. The existence of pores and their opening duration were ascertained by incubating printed cells with fluorescently labelled g-actin monomers. The monomers got internalized by the cells through the nanopores for up to 2 h. As actin is a fundamental part of the cytoskeletal system, research like these are also useful for the study of cytoskeletal dynamics and cellular mechanics through fluorescence imaging and tracking of the monomers inside the cells.

3.2. Piezoelectric inkjet printing based research

Apart from thermal inkjet printing, the piezoelectric inkjet printing has also been shown to cause formation of transient nanopores on the cell membranes. Barui et al. [22] printed 3T3 mouse fibroblast cells and assessed the nanopore formation, cell membrane integrity, cell viability and cell proliferation. Similar to other research results, the authors found no significant difference between the cell viability of printed cells and the non-printed control cell populations. However, the cell proliferation rate of the printed cells was found to be lower than that of the non-printed control. Analysis of cell membrane integrity or pore formation was done by assessing the cellular penetration of the molecular probes propidium iodide and Texas Red labelled dextran, similar to the previously explained research [42] and as illustrated in Fig. 3 (b). The researchers also noted that printing cells with gradually increasing voltage of piezoelectric actuation, in the range of 80–100 V, led to

gradually increased uptake of dextran, prolonging even beyond 2 h, unlike in other research. However, it was found that dextran with smaller molecular weights (3 kDa, 10 kDa) had higher uptake than higher MW dextran (40 kDa, 70 kDa). The main finding in this research was that at higher voltages, there are more number of pores with higher retention time but with smaller diameters, compared to the pores formed at lower voltages. The researchers hypothesise that there are multiple factors driving pore nucleation and growth which would require further extensive research in order to be identified.

The aforementioned experiments have paved the way for inkjet printing technology to be established as a novel and prominent method of transporting desired foreign biologically active molecules, such as DNA, peptides and therapeutics, up to a certain size, inside the cells. However, while promising, inkjet cell printing has been applied for intracellular delivery and transfection by a very limited number of research groups, most probably due to a lack of systematic controllability on the amount of thermal and mechanical stresses delivered to the cells.

4. Gene expression modification

Since 2019, there has emerged an interest in studying the previously unknown effects of thermal and mechanical stresses, occurring during the inkjet cell printing process, on gene expression and cell metabolism. A very high post-printing cell viability may not mean that the thermal and mechanical stresses do not cause subtle changes in the gene expression and the biochemical processes of the printing cells, particularly the sensitive ones, such as stem cells. As elaborated in one of the previous sections, substantial research has been conducted to study the effects of thermal and piezoelectric inkjet printing on cell viability with largely optimistic conclusions. But, until recently none of this research has assessed the integrity of cellular processes and functions at the

transcriptome level.

4.1. Thermal inkjet printing based research

In one of the first examples of such research addressing this issue, Solis et al. [43] assessed the effect of thermal inkjet printing on the cellular pathways of human microvascular endothelial cells (HMVECs) and confirmed the activation of VEGF pathway of angiogenesis. HMVECs suspended in calcium chloride ($CaCl_2$) solution were printed into Petri dishes pre-filled with cell culture medium and the expression of six specific cytokines with angiogenic effects were measured in the printed cells using multiplexed magnetic bead immunoassays. The expression levels of heat shock protein 70 (HSP70), interleukin 1α (IL-1α), vascular endothelial growth factor A (VEGF-A), interleukin 8 (IL-8), and fibroblast growth factor 1 (FGF-1) were found to be significantly higher than their expression levels in the manually pipetted or non-printed cells. The angiopoietin 2 (Ang-2) expression was also found to be slightly higher in the printed cells, yet with a non-significant difference than that in the non-printed cells. Additionally, the proteome phospho-kinase array immunoassay revealed that the expression of HSP27 and HSP60, both of which help in angiogenesis, were also significantly higher in the printed cells. These results indicate that thermal inkjet bioprinting has the potential to induce angiogenesis in the vascular endothelial cells as illustrated in Fig. 4 (a). Apart from the biochemical changes, the printed cells also showed morphological changes in size and became 2–3 times elongated than the non-printed cells which is also suggestive of the initiation of cellular pathways that cause angiogenesis. Further research in this area has the potential to contribute significantly to solving the long-standing issue of lack of vasculature in the *in vitro* bioprinted tissues [94,95] destined for implantation.

While applying thermal inkjet bioprinting to develop a 2D and 3D model of MCF07 breast cancer cells for drug discovery applications, Campbell et al. [44] discovered that the bioprinted MCF-7 cells showed a viability of 8.2–10.8% on exposure to Tamoxifen, an anti-breast cancer drug. The manually seeded cells, in comparison, showed a viability of only 0.05–0.11%. The authors hypothesised that the unexpected higher survival rate of printed cells may occur due to the activation of the chaperone proteins, such as HSP70 and HSP90, due to the thermal stress during the inkjet process. These HSPs or heat shock proteins act to protect the cells against heat or chemical stresses and their over-expression is a hallmark of cancer cells causing their enhanced

survivability and proliferation [96,97]. This causes the bioprinted MCF-7 cells to exhibit a biologically more relevant *in vivo* cancer cell like model in comparison to the manually seeded cells. Working further on this finding, Campbell et al. [45] extensively assessed changes in the gene expression patterns of bioprinted MCF-7 cells in comparison to the non-printed control. On analysis through the phospho-MAPK antibody array, the bioprinted cells showed kinase phosphorylation at 21 sites in comparison to 11 sites in the non-printed cells as shown in Fig. 4 (b). On relating these phosphorylated sites or targets to cellular processes, they were found to be interacting with the pathways for intracellular signal transduction, signal regulators, response to stress and apoptosis. This clearly means that the occurrence of these cellular processes is enhanced after thermal inkjet printing of the cells due to the activation of various proteins by kinase phosphorylation. Also comparatively, 266 genes were upregulated while 206 were downregulated in the printed cells, some of which are graphically represented in Fig. 4 (c). In addition, 5 genes, namely, NRN1L, LUCAT1, IL6, CCL26, and LOC401585 were exclusively expressed only in the printed cells. However, there were no genes which expressed in the non-printed cells and not in the printed cells. The authors then identified the gene ontologies in the cellular functions and components of the 5 genes that expressed only in the printed cells. The genes were found to be variably associated with protein binding, catalytic activity, molecular function regulation, molecular transducer function, plasma membrane, extracellular region, and cellular response to stimulus, regulation, localization and processes. Among those genes which were upregulated in the printed cells, the important ones, with more than 10 protein-to-protein interactions, were CYP1A1, IL6, UGT1A6, EGFR, and CYP1B1. In addition, the genes CYP1A1 and CYP1B1, which code for the important cytochrome P450 enzymes, were upregulated by 300-fold and 10-fold, respectively. Apart from catalysing steroids, fatty acids and xenobiotics, cytochrome P450 enzymes may also cause DNA damage from their catalytic production of highly reactive intermediates, thus, contributing to tumour formation [98]. Among the downregulated genes, with 10 or more protein interaction, were TP53, FOS, JUN, EGR1, HIST2H2AC, and FOSB. Among these, the TP53 is a well-known tumour suppressor gene. The upregulation of cytochrome 450 genes and the downregulation of TP53 further explains why the authors observed enhanced survival of the MCF-7 cells in their previous study [44]. All these results suggest the capability of thermal inkjet printing to cause large scale variations in genetic expression.
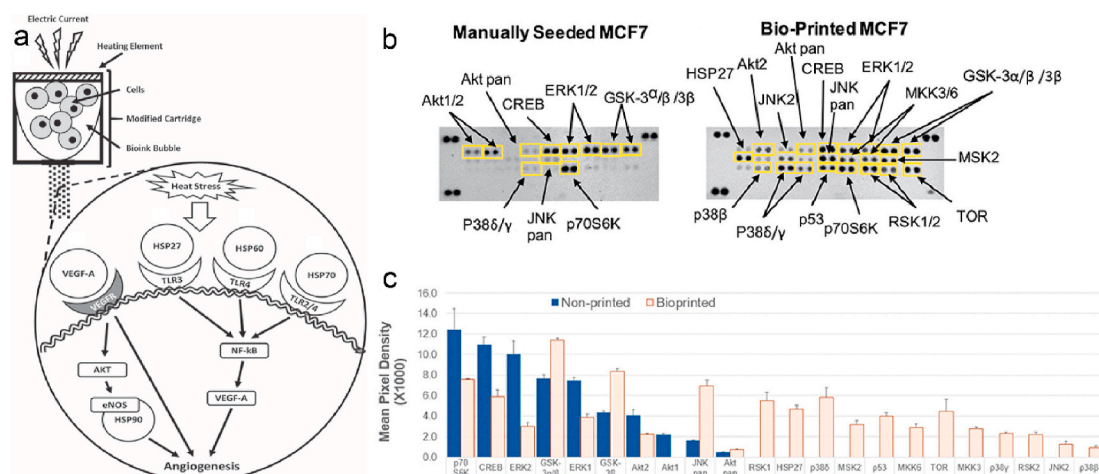
Fig. 4. (a). Schematic illustration of activation of cellular pathways that cause angiogenesis due to the thermal and mechanical shock on the human microvascular endothelial cells (HMVECs) caused by thermal inkjet bioprinting. [image (a) republished with permission from Ref. [43] Copyright © 2019 IOP Publishing Ltd]. **(b–c)** Alteration in gene expression and subsequent activation of cellular pathways after inkjet cell printing. **(b)** Phospho-MAPK antibody array showing the sites of occurrence of kinase phosphorylation in non-printed (manually seeded) and printed MCF-7 cells. **(c)** Comparison of expression of selected genes in non-printed and printed MCF-7 cells. [images (b–c) republished with permission from Ref. [45] Copyright © 2020 Campbell, Mohl, Gutierrez, Varela-Ramirez and Boland].

4.2. Piezoelectric inkjet printing based research

The aforementioned experiments have all been conducted with thermal inkjet printers. As, unlike thermal actuation, piezoelectric actuation causes only mechanical stress, it is essential to know the difference which occurs in the effects on gene expression of the printing cells between the two printing methods. Yumoto et al. [46] used a custom-made piezoelectric inkjet actuator to dispense mouse embryonic stem cells (mESCs) and test the genetic integrity through RNA sequencing in addition to the cell viability assays. The cells, suspended in mESC-specific culture medium, were also dispensed manually with micropipettes for comparison. Conventional cell viability evaluations 48 h post-dispensing showed cell survival of >90% in both manually-dispensed and inkjet-dispensed samples. The cell proliferation from 12 h to 48 h post-dispensing increased by about 12 times for both manually-dispensed and inkjet-dispensed samples. On inducing differentiation of the embryo bodies (EBs) of mESCs, both manual and inkjet dispensed samples showed gene markers *Gata6*, *T* and *Sox1* for endoderm, mesoderm and ectoderm, respectively, and a high expression of marker for embryonic stem cells, *Dppa5a*, at all time points post-dispensing, indicating a maintenance of pluripotency and the ability to differentiate into all three germ layers. On conducting RNA sequencing analysis, more than 10,000 genes were detected to be expressed in both manual and inkjet dispensed cells at various time points post-dispensing and without any significant differences in the expression levels between the two methods. These results indicated a close similarity in the mechanical stress between manual dispensing and the custom-made piezoelectric actuator. A few genes showed differential expression at different time points and the expression levels of some of them were significantly different between the manual and inkjet dispensed cells. Compared to the manually dispensed cells, the inkjet cells showed at 24, 48 and 72 h post-dispensing, an upregulation of 29, 166 and 25 genes, respectively, and a downregulation of 57, 15 and 35 genes, respectively. The overall inference in this study, thus, was that piezoelectric inkjet printing mostly does not cause significantly different effects to cell integrity than manual dispensing. As manual dispensing has to be carried out for passaging cells in any cell culture-based experiment, all the cells get imperatively subjected to the mechanical stress that it causes. In this regard, if the viability and gene expression results are not significantly different between manually-dispensed and inkjet-dispensed cells, then it insures piezoelectric inkjet printing as a safe method for cell printing.

The data obtained in these recent studies confirm that thermal inkjet bioprinting elicits a heat shock response in the cells leading to a sudden over-expression and under-expression of several genes which, in turn, leads to alterations in cellular processes and pathways. Again, however, more research in this area and subsequent improvements in the inkjet bioprinting engineering are required to be able to precisely control and manipulate cellular biochemistry *in vitro* by means of physical factors, such as heat and mechanical force. These studies also suggest that if the purpose of cell inkjet printing is anything other than gene expression modification, or if any change in the normal gene expression would affect the intended results and purpose of cell printing, then thermal inkjet printing may not be suitable and piezoelectric inkjet printing should be relied on.
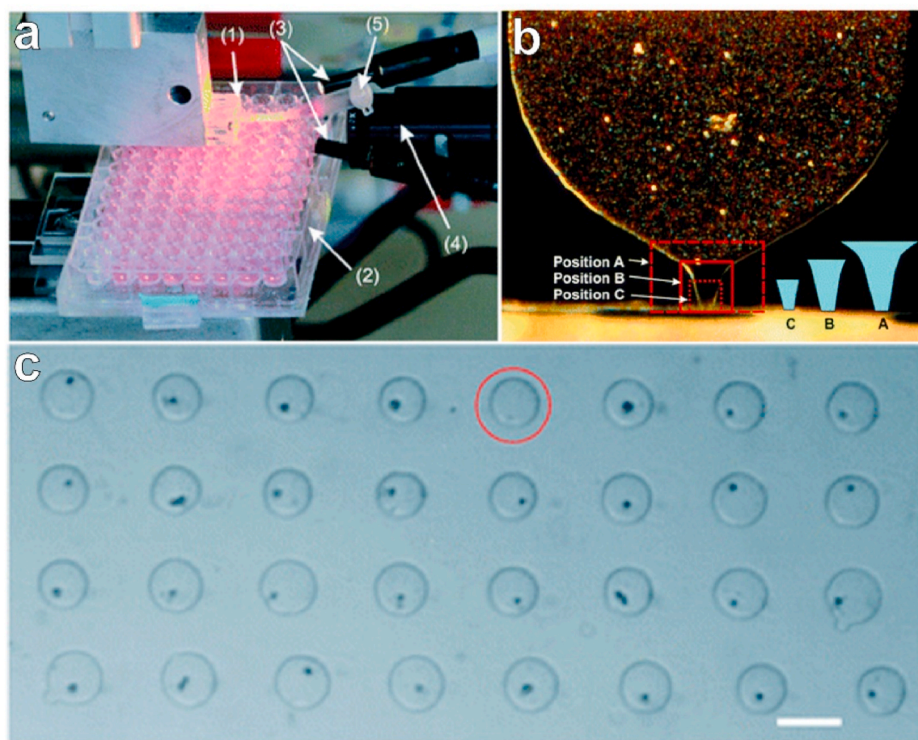
5. Single cell sorting

Single cell sorting refers to the physical separation of individual cells, based on number, from a homogeneous or heterogeneous cell population. Single cell sorting is essential for building cell arrays and cell-based lab-on-a-chip devices which are applied in a number of biomedical research, such as single cell analysis, single cell PCR, high throughput drug screening, stem cell research, and production of clonal cell lines [47,48].

5.1. Existing techniques and initial trials with inkjet printing

While conventionally, flow cytometry techniques and microfluidic devices are used for cell sorting, they are more suitable for the purification of heterogeneous cell populations based on their physical characteristics, such as cell type, size, morphology and surface protein expression [28,99–102], rather than separating cells by number and depositing one or a fixed number of cells at a time on a substrate. Also, these methods of cell sorting may lead to a much reduced cellular viability due to labelling and much prolonged fluid shear stress compared to inkjet printing [28,101,103]. Inkjet bioprinting, therefore, is more suitable for a relatively simpler job of separating cells based on number and depositing one or a pre-determined number of cells at a time. Jetting as low as one cell at a time remained a challenge until Nakamura et al. [24] were able to generate inkjet droplets with bovine vascular endothelial cells, suspended in cell culture medium, and obtain 1–4 cells, at random, per deposited droplet or dot. The authors concluded that the number of cells in a dot is dependent on the cell suspension concentration, which was 1–1.5 million cells per mL for obtaining 1–4 cells per dot, with a few dots going blank with no cell. Consequently, the number of shots per dot or the jetting frequency was also found to determine the final number of cells in a dot. In another work, Xu et al. [47] were able to sort one to several insulin producing beta-TC6 cells, suspended in sodium alginate, and print them into calcium chloride solution to form cell-laden microparticles of 30–60 μm in diameter at a very high speed of 55,000 microparticles per second, using a modified commercial thermal inkjet printer. The printing parameters, such as the concentrations of cells, alginate and calcium chloride, affected cell distribution or cell number in the microparticles. The cells demonstrated 89% viability 1 day after printing and continuous insulin secretion and maintenance of normal cellular function for 6 days of the post-printing observation period. The authors, thus, developed a high throughput method of inkjet printing based cell sorting. In these early works, even though the researchers were able to generate single-celled droplets or particles, the number-specific cell sorting was an uncontrollable phenomenon and, therefore, they failed to precisely print one and only one cell per droplet throughout the printing process.

5.2. Attaining high precision

The capability of controlled single cell inkjet printing developed when research progressed into integrating sophisticated camera and image processing systems in the inkjet printer for dispensing a droplet only when it is observed to be containing a single cell. In one of the first such research, Yusof et al. [28] have developed a single cell manipulator (SCM) system, similar to a piezoelectric inkjet printer, for the isolation of single cells, generation of cell-containing droplets and deposition of the droplets on a substrate, as shown in Fig. 5 (a). The SCM consists of a transparent dispenser chip made of silicon and glass and is driven by a piezoelectric actuator, jetting the droplets in the range of 150–800 pL in volume. A CCD camera is used for optical imaging of a region of interest (ROI) at the nozzle of dispenser chip, as shown in Fig. 5 (b), to detect single cells through an image recognition algorithm before dispensing the droplets. This ROI is analysed by an optical particle detection mechanism and a sorting algorithm so that a droplet is dispensed only when there is only one cell in the ROI. For testing their SCM system, the researchers dispensed HeLa cells, suspended in minimum essential medium eagle (MEM eagle), on glass slides and on 96-well microplates followed by incubation for cell growth. The effect of ROI size, ROI location and cell suspension concentration were also analysed. A high dispensing efficiency, measured as the droplets containing only one cell each, of up to 87% was achieved, as shown in Fig. 5 (c) and it was found to decline on increasing the cell concentration beyond 5.3×10^5 cells/mL. Similarly, a volume of 400 pL per droplet was found to be optimal for generating single cell containing droplets. As a low actuation force causes droplet malformation and a high actuation force causes

Fig. 5. (a) For single cell sorting, cell printing is conducted with an inkjet-like single cell manipulator system, consisting of (1) dispenser chip, (2) 96-well plate as substrate, (3) illumination source, (4) CCD camera objective lens, and (5) bioink reservoir. **(b)** Three different regions of interest (ROI) shown as positions A, B and C are compared for determining the most efficient ROI in giving only one cell per droplet, that is, if there is only one cell in that ROI then the droplet can be dispensed with the assurance that the dispensing droplets also give only one cell per droplet. **(c)** Micrograph of a printed sample showing only one cell in one printed dot, with the red circle showing a void dot resulting from marginal printing error (scale bar: 200 μm). [image republished with permission from Ref. [28] Copyright © 2011 The Royal Society of Chemistry]. (For interpretation of the references to color in this figure legend, the reader is referred to the Web version of this article.)

mechanical stress on the cells and reduces their post printing viability, the actuation velocity of 40 μm/s with 8 μm actuator displacement was found to give the highest viability yield of 75% in the seeded single cells. In another instance of development of a single cell sorting inkjet printing system, Gross et al. [48] used a similar single cell printer consisting of a piezoelectric transparent dispenser chip attached with a high magnification camera and an automatic cell detection system. The cell detection system constitutes a set of algorithms which differentiates between droplets and classifies them as droplets containing only one cell and droplets containing no or more than one cell. If the dispensed droplet does not contain exactly one cell, it is instantaneously withdrawn by a pneumatic shutter system consisting of a vacuum pump, a high speed magnetic valve and a tubing just behind the nozzle orifice. Five cell lines, namely, human cervical cancer cells (HeLa), mouse embryonic fibroblasts (NIH-3T3), human dermal fibroblasts (H-FIBD), human keratinocytes (H-KER), and turboGFP-transfected human osteosarcoma cells (U2OS), all suspended in PBS solution, were printed separately into microwell slides preloaded with culture medium. Across all cell types, 77–94% of the wells contained only one cell and the cell viability rates were 89–98% at 24 h post-printing. The printing of fluorescent U2OS also helped evaluate printing performance. A single cell was detected and printed in approximately 10 s, taking around 3 min to fully print a slide of 18 wells with single cells, with a final yield of 94% and cell viability of 90%. Thus, using various cell lines, the authors demonstrated the ability of inkjet printing to sort and print different kinds of mammalian cells. In another example of improvement in single cell sorting, The et al. [49] developed a one cell per droplet system of inkjet printing by building an automated cell detection system for observing the cell positions inside the nozzle or tip of the jetting device and processing their images. The researchers used SF9 insect cells with a mean size of 21 μm and suspended at 1 x 10^5 cells/mL concentration in physiological saline. The piezoelectric inkjet process was programmed in such a way that a droplet forming inside the nozzle was ejected at the printing location only if the automatic cell detection and image processing system detected one cell in the droplet. If the droplet contained no cell or more than one cell, then the printing location is changed to a

discard location and the droplet is ejected out. Using this automated system, a high success rate of 98% was achieved in obtaining only one cell per dot.

5.3. Exploring applications

With good progress and increased accuracy in single cell sorting using inkjet printing, its potential for out-of-lab biomedical applications are being explored. Stumpf et al. [50] showed one such example which was single cell polymerase chain reaction (PCR) to amplify whole genome of single cells, printed by a single cell printer similar to the one described previously and shown in Fig. 5 (b). Human B-lymphocytes of Raji cell line were cultured, suspended in PBS solution and printed directly into standard PCR tubes. The nozzle of the transparent piezoelectric dispenser chip was optically scanned for detecting single cells each time before dispensing to ensure printing of single cell containing droplets only. Post-printing observation revealed that 17 out of 20 cells retained spherical shape and normal morphology. Real time PCR from truly single cells yielded a 33% success rate or 65 out of 197 cells. Afterwards, a whole genome amplification (WGA) was performed to amplify all the cell's DNA >1000 times, which yielded a 64% success rate or 21 out of 33 cells in real time PCR. The PCR yields were low but in expected numbers as PCR tests are affected by a number of different factors, such as loss of single cell in centrifugation and loss of target DNA in the processing steps. The authors, thus, showed an automated process for dispensing and loading single cells in reagent vessels for successful downstream single cell real time PCR. Another potential out-of-lab application was demonstrated by Yoon et al. [51] who printed single tumoral cells in microwell plates and assessed them in high throughput fashion to discover heterogeneity among the cells. Patient-derived urinary bladder cancer cells were suspended in and precisely printed on 384-well plates using a piezoelectric inkjet printer. After *in vitro* culture in the microwell, the single clonal cells developed into organoids which were proliferated further in matrigel for 7–14 days. RNA was then extracted from the cells for reverse transcription and obtaining cDNAs, which were subjected to qRT-PCR. Gene expression analysis revealed

high degree of variability in the presence of mRNA of luminal-type marker genes, such as UPK1A, UPK2 and FOXA1, and basal-type marker genes, such as KRT5, KRT14 and KRT6A. Additionally, treatment of single cell derived organoids with cisplatin, an anti-cancer drug, showed differential expression of the apoptotic marker caspase-3, ranging from 2.7 to 35.8%, suggesting the presence of heterogeneous clones, with some clones showing resistance. Detection and identification of such clones are essential to prevent the drug-resistant ones from causing tumour relapse after chemotherapy. The authors, thus for the first time, showed the utility of inkjet bioprinting in sorting and detecting intratumoral heterogeneity or the presence of several clones within the same tumour.

Though the actual number of cells inside a forming droplet cannot be controlled, the inkjet printing systems discussed here allow an easy and label free detection and printing of single cells. Thus, over the years, inkjet bioprinting has developed into a sophisticated and accurate tool for single cell sorting. This, in turn, has opened the doors for further applications that require precision single cell seeding, such as cell microarray and cell micropatterning.

6. Cell microarray

A cell microarray is an analytical tool having several different types of cells deposited in well-organized rows on a substrate, often called as a chip or lab-on-a-chip, for performing high-throughput and multiplexed biomedical assays or biosensing [104]. The advantage of cell microarrays is that several different analytes, such as therapeutics, antibodies, lipids, peptides, enzymes, and other molecules, can be analysed on a wide phenotype of cells at once [104,105]. Another important significance of cell microarray is the effective miniaturisation of conventional assay methodologies for medical diagnostics of various diseases [106]. This not only helps minimise sample size of scarce analytes and expensive reagents but also makes the diagnosis process faster, efficient and portable [52,105]. Additionally, in cell biology, cell microarrays can be applied to study cell-cell interactions, cell interactions with their microenvironment and cellular mechanics and physiology under different conditions and stimuli [107].

6.1. Current research

As inkjet bioprinting is establishing itself as a prominent tool for direct and non-contact cell printing and single cell sorting, it helps in very fast and easy fabrication of cell microarray based lab-on-a-chip devices and bioMEMS [28,49,106]. However, one important issue with cell microarray is the quick drying up of the freshly printed culture medium dots, containing the cells, owing to their picolitre volume [29, 105]. This necessitates the printed array to be used for analytical studies within minutes or else risk obtaining either misleading data or no data at all. Another challenge is the spreading out of the dots or cell migration from one location to another leading, again, to false assay or biosensing results [29,105]. In order to overcome these challenges, Liberski et al. [29] adopted a new approach to fabricating cell microarray with dual liquid phase system as shown in Fig. 6. The authors first printed dots of culture medium at specific locations on a substrate and simultaneously spread a thin layer of an oxygen-permeable mineral oil, in their case paraffin, evenly all over the substrate. Afterwards, mouse L929 immortalized fibroblast cells were printed on top of the culture medium dots already submerged under a thin layer of the oil. The cells traversed through the oil layer and sank at the bottom of the dots where they remained alive for several hours, as indicated by the >90% cell viability 7 h post-printing. The non-volatile oil in this biphasic system prevented the culture medium from drying out. This approach makes the cell microarray chips more practicable for such biosensing or assay applications which require prolonged experimentation of up to a few hours before the required results can be obtained. Additionally, the hydrophobicity of oil assures that the dots with cells in them do not spread out, thus maintaining the integrity of the microarray design.

6.2. Attaining high precision

With ongoing design and operational advancements, inkjet bioprinting is now capable of printing not only one cell per droplet but also a fixed number of more than one cell per droplet, as per the requirement. To demonstrate the feasibility of inkjet bioprinting in building a live cell microarray with very high precision in cell number per printed dot, Jonczyk et al. [52] used a commercial piezoelectric inkjet cell printer (Nano-Plotter NP2.1) to fabricate a microarray of A-549 human lung cancer cells, suspended in DMEM with 10% FCS before printing. Around 1200 cells per dot were printed in an array with a very low spot-to-spot variation of ±8.6 in cell number. After printing and culturing the cells for 3 days in a humidified environment, the authors observed a high cell viability of up to 88%. Elsewhere, Park et al. [53] developed a cancer microtissue co-culture array by piezoelectric inkjet printing cancer cells on nanofibrous membrane with embedded fibroblasts. Firstly, CCD-1112SK fibroblasts were grown on top of nanofiber membranes which were fabricated by electrospinning polycaprolactone solution and placed in 96-well plates to act as substrate for cancer cell printing. Then, HPV18-positive HeLa cervical cancer cells, suspended in DMEM with 0.5% collagen, were printed in the wells, with 150 droplets in each well, achieving an almost 100% cell viability as observed immediately after
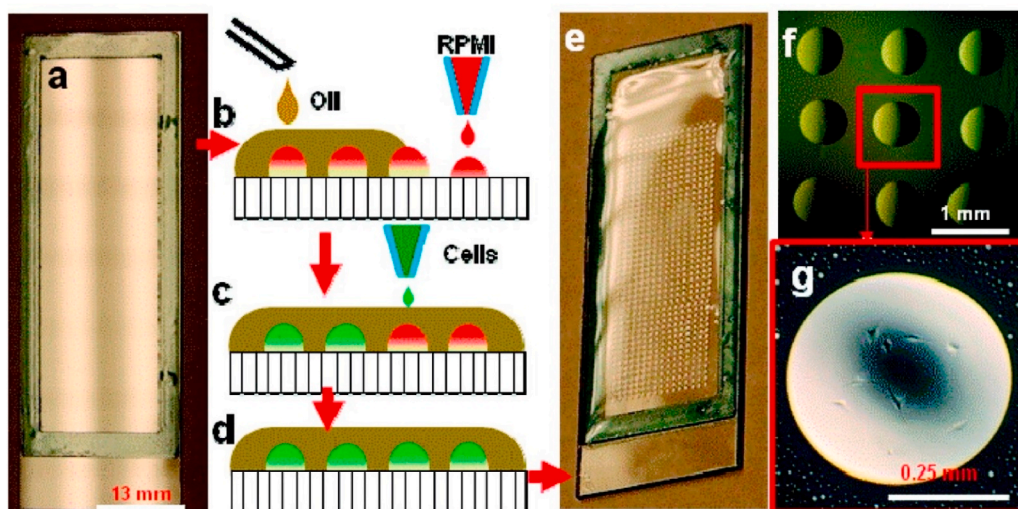
Fig. 6. Stages of cell microarray fabrication. **(a)** glass slide substrate with sealing frame along the edges to prevent oil spillage, **(b–d)** printing of culture medium, spreading of paraffin oil and printing of L929 cells, **(e)** substrate with fully printed microarray, **(f)** a micrograph of microarray units (scale bar: 1 mm), **(g)** a micrograph of a printed dot containing cells after 7 h of incubation (scale bar: 0.25 mm). [image republished with permission from Ref. [29] Copyright © 2010 American Chemical Society].

printing. The deposited cancer cell aggregates increased in size due to cell proliferation, while maintaining their shape, similar to *in vivo* tumours, for up to 7 days post-printing. Also, the matrix metalloproteinases MMP2 and MMP9, which are the hallmarks of invasive cancers, were found to be upregulated in all the microtissues. These results showed the robustness of the method in developing an inkjet bioprinted *in vitro* cancer model.

An even more precise and smaller scale microarray was fabricated by Mi et al. [54] who developed a novel piezoelectric cell printing system with a high printing position accuracy of 10 μm which ensured printability in tiny microwells, and a low droplet volume of 0.1 nL which ensured single cell dispensing ability. Single GFP-transfected MDA-MB-231 human breast cancer cells and single RFP-transfected human umbilical vein endothelial cells (HUVECs), suspended in different culture media, were printed on a microfluidic chip 22 × 22 mm in size and consisting of an array of 400 microwells, each measuring 200 μm in depth and 300 μm in diameter. Up to 70% of droplets contained single cells on performing the printing at 90 V with 75 μm diameter nozzle and 1×10^6 cells/mL bioink concentration. The whole microfluidic chip platform was kept in an ice tank, without submerging the top printing area, to prevent the droplets in the microwells from drying out. The printed cells showed normal growth and migration such as surface adherence, migration to the sides of the wells and spindle formation and more than 87% viability 7 days post-printing. Additionally, incubating the cancer cells with paclitaxel caused inhibition of cell growth and migration and hindrance of normal cellular shape and morphology. The authors, thus, developed a new inkjet bioprinting based platform for multicellular printing and high throughput single cell analysis and drug screening.

In these research studies, the accurate drug screening results with known drugs show promise of mitigating the high failure rates of human clinical trials of those new under-trial drugs which have successful preclinical testing results in conventional assays and animal models but do not accurately represent human *in vivo* conditions.

7. Cell micropatterning

Cell micropatterning is the deposition of cells in a pre-determined 2D or 3D pattern on a substrate or scaffold to mimic the complex *in vivo* tissue architecture with micrometre scale resolution for various purposes, such as drug screening and tissue engineering. Alongside cell microarray models, micropatterned cells are applied to establish the foundation of cell-based biomedical micro-electro-mechanical systems (bioMEMS), organ-on-a-chip models and point-of-care (PoC) devices for personalized medicine [108]. Additionally, in cell biology, cell micropatterning is applied to investigate multi-cell interactions, cytoskeleton mechanics, cell axis and symmetry during division and differentiation, cell migration and the effects of environment and stimuli [109,110]. Cell micropatterning, thus, is the miniaturised deposition of more than one type of cells on a substrate based on a pre-determined 2D or 3D geometry. The concept of utilizing inkjet printing for cell micropatterning, albeit indirectly, was developed in the 1980s when cell adhesion molecules and monoclonal antibodies were inkjet printed in pre-defined patterns on a substrate, upon which, culturing of cells resulted in growth of specific cells only on those specific patterned locations due to specific cell adhesion [111]. This method was called as cytoscribing and the cellular patterns thus obtained as cytoscripts. Cytoscribing was one of the most important steps towards the development of the first direct inkjet printing of cells. Deposition of different cells in required configuration is a step forward to generate organoids *in vitro*, called as organ-on-a-chip, for mimicking *in vivo* organs [108]. The resulting structures act as disease models for drug screening and has the potential to lay the foundation for *in vitro* organ biofabrication for organ transplantation [19].

7.1. 2D micropatterning

In one of the first such studies, Xu et al. printed rat primary embryonic motor neurons [55], hippocampal neurons [56] and cortical neurons [56], all suspended in DPBS solution, with a modified commercial thermal inkjet printer. The cells were patterned as separate circles on the substrates, which were carefully incubated with culture medium for cell proliferation and differentiation. The circular pattern facilitated the motor neurons in forming a neural ring within 2 days of culture and forming dendritic extensions by the 7th day. The hippocampal and cortical neurons also started showing differentiation and neuronal ring formation within a day of seeding and developed extensive processes by the 13th and the 9th day, respectively. Such printed neuronal models have the potential to be used to study brain diseases, such as epilepsy [25]. In another research, Park et al. [30] have demonstrated the printing and patterning of mammalian cells onto a liquid-filled substrate, a culture dish filled with culture medium. The researchers used a piezoelectric inkjet printer to print NIH3T3 mouse fibroblasts and HEK293A human kidney cells, suspended in culture medium, first as dots to determine positional accuracy in a liquid environment and then as different patterns for co-culturing the printed cells, as shown in Fig. 7 (a). As the droplet containing the cells plunges into the culture medium in the dish as illustrated in Fig. 7 (b), the impact force causes the cells to deviate from their pre-defined positions as they sink in the medium and adhere to the bottom of the dish. For solving this issue, the authors adjusted the printing parameters and obtained a minimum best positional error of ±66 μm. For this, the optimal printing parameters, as used by the authors, were the stage movement speed of 5 mm/s, the nozzle-substrate distance of 1 mm and the culture medium volume of 3 mL in the dish. This bioprinting strategy is also one of the approaches to eliminating the risk of quick drying up of the printed dots and can, thus, be beneficial not only for cell micropatterning but also for cell sorting and cell microarray fabrication. Afterwards, the cells were printed in various geometric shapes with fine edges for co-culturing. The authors were also able to print the cells in complex patterns with cell concentration gradients rather than hard boundaries as shown in Fig. 7 (c), thus resulting in a 2D architecture of co-cultured *in vitro* cells that mimics natural tissues even more closely.

7.2. 3D micropatterning

Research has also furthered into 3D cell micropatterning, which either requires separate layers of a gel-like support material to be printed alternately with the directly printed cells [56,57], or requires printing of cells suspended in a liquid cross-linker onto a crosslinkable scaffold precursor [58,59]. One early example [56] of alternate printing of cells and scaffold is for the fabrication of multi-layered neural sheets by thermal inkjet printing. NT2 neuronal precursor cells suspended in DPBS were printed layer-by-layer alternating with a layer of fibrinogen and thrombin which yielded a fibrin gel layer. The sandwiched cells showed even distribution, anchorage to scaffold fibres with filopodia, and development of neurites within 12 days of *in vitro* culture, thus, forming neural sheets which measured 25 x 5 × 1 mm in dimensions. Such neural constructs provide a vital tool for the clinical study of treatment of neural injuries and degenerative diseases. Similarly, an early example [58] of co-printing of cells with a scaffold precursor is for the fabrication blood vessel like tubular structures using a modified commercial thermal inkjet printer. Human microvascular endothelial cells (HMVEC) suspended in thrombin and DPBS were printed on a fibrinogen containing substrate to form a rectangular grid of fibrin tubes around 100 μm in diameter with embedded cells. The cells showed alignment, proliferation and confluence on the inner lining of the micron-sized 3D fibrin channels, thus, mimicking angiogenesis and forming blood capillaries during the 21 days of *in vitro* culture.

More intricate examples of 3D cell micropatterning involve co-printing and subsequent co-culture of multiple cell types, thus forming
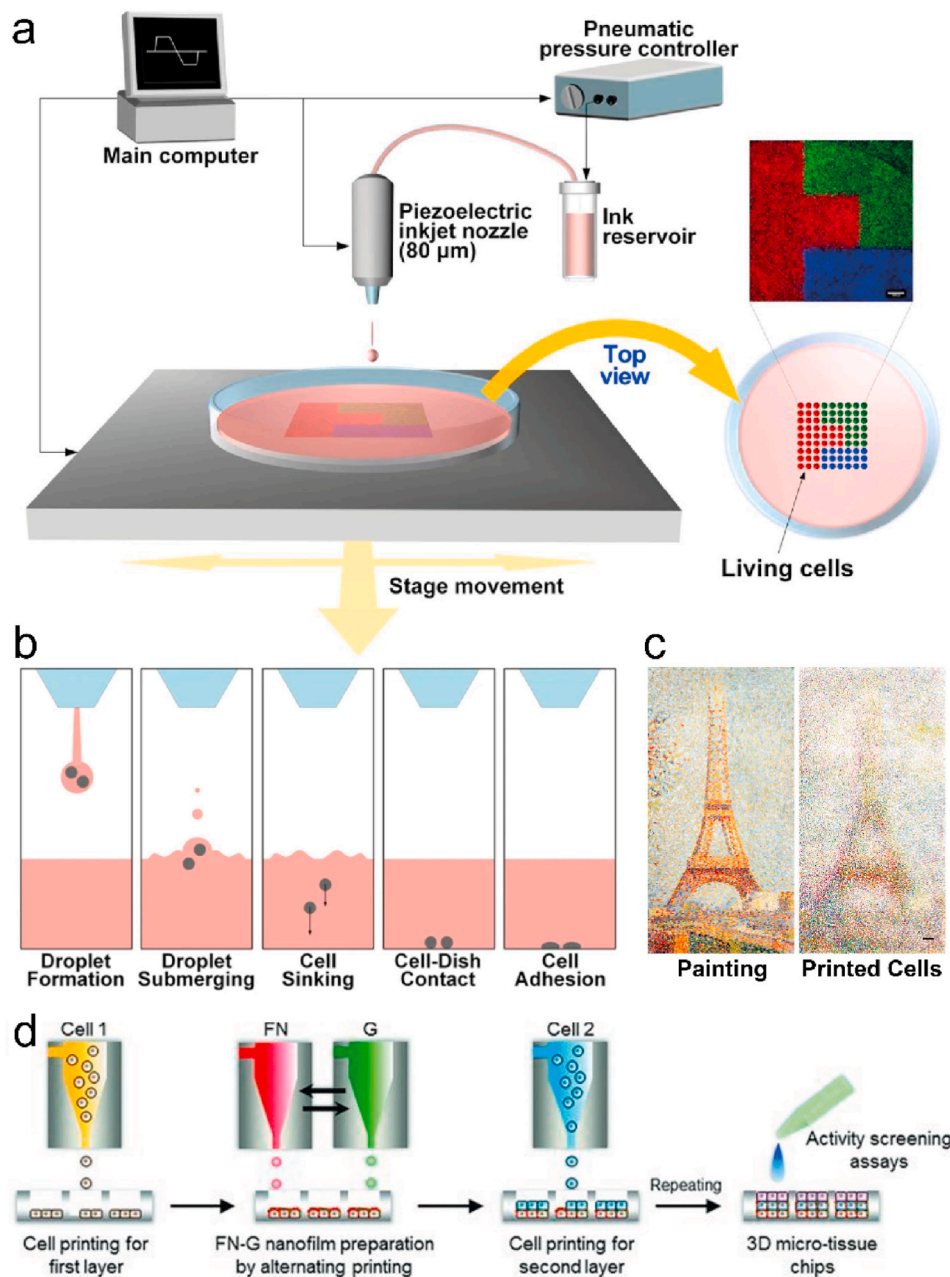
Fig. 7. Schematic illustrations of **(a)** cell printing in a liquid substrate to create cellular micropatterns, and **(b)** the cellular voyage from the inkjet nozzle to the bottom of the culture dish after traversing through the liquid culture media. **(c)** Cell density-controlled printing, based on an Eiffel Tower painting as design source, to create micropatterns with cellular gradient, as imaged with the help of three different fluorophores (scale bar: 1 mm). [image republished with permission from Ref. [30] Copyright © 2017 Springer Nature]. **(d)** Schematic illustration of step-wise construction of a liver-on-a-chip model by 3D cell micropatterning and subsequent testing of effect of different drugs, cosmetics and chemicals. **Cell 1:** Endothelial cells (HUVEC); **FN:** Fibronectin; **G:** Gelatin; **Cell 2:** Hepatocytes (HepG2). [image republished with permission from Ref. [57] Copyright © 2013 WILEY-VCH Verlag GmbH & Co. KGaA, Weinheim].

more complex constructs. Matsusaki et al. [57] developed a 3D liver-on-a-chip with different layers of hepatocytes and endothelial cells, the two most abundant cells in liver, as a model for drug and cosmetics screening and evaluation assays and an alternative to the use of animal models. Human hepatocellular carcinoma cells (HepG2) and human umbilical vein endothelial cells (HUVEC) were printed as single (HepG2), double (HUVEC/HepG2), and triple (HUVEC/HepG2/HUVEC) layers in 440-microwell plates, as shown in Fig. 7 (d), by a commercial piezoelectric inkjet printer (DeskViewer) for high throughput evaluations and to investigate the effect of cell-cell interactions. Fibronectin and gelatin layers were printed in between the cell layers to mimic the extra cellular matrix. The liver microtissues, thus formed, were incubated for 2 days and evaluated by liver function tests which revealed CYP3A4 and albumin secretions as confirmed by fluorescently labelled antibodies. Normal liver function was also confirmed by degradation of Vivid red enzyme to resorufin by CYP3A4 enzyme. For hepatotoxicity assay, the microtissue was incubated with troglitazone for 2 days, after which, the 3-layered microtissues showed higher cytotoxicity than single and double layered ones. Overall, with increasing the number of layers, the fluorescence intensities indicating albumin secretion, CYP3A4 secretion and CYP3A4 activity also increased successively. As liver plays a central role in metabolism, liver-on-a-chip based devices are going to become essential clinical and industrial tools and in such a scenario, inkjet bioprinting offers a very easy and fast route to construction of such devices.

A more complex, hybrid and multi-layered patterning of different mammalian cells was shown by Xu et al. [59] who fabricated a three cell composite hydrogel structure using a modified thermal inkjet printer. Human amniotic fluid-derived stem cells (hAFSCs), canine smooth muscle cells (dSMCs), and bovine aortic endothelial cells (bECs) were suspended in calcium chloride in three separate cartridges and printed simultaneously on separate pre-determined locations on a sodium alginate and collagen composite solution. Several layers of printing and alginate cross-linking resulted in formation of hybrid 3D hydrogel with

three cell types, thus, resembling a cross-species or chimeric tissue model. The circular hydrogel measured just under 1 cm in diameter with a half of the area covered by bECs, a quarter of the area covered by dSMCs and the remaining quarter of the area covered by hAFSCs. On 7-day *in vitro* culture, the cells showed anchorage to the scaffold, high viability of >90%, normal proliferation, and normal physiology and phenotypic expression. After 3-day *in vitro* culture, the construct was implanted subcutaneously in athymic mice for 2 weeks, after which the cells showed high viability and remained at their original locations within the hydrogel. Also, owing to their different functions, the hAFSCs, dSMCs and bECs were tested for differentiation, electrophysiology, and vascularization, respectively, immediately after printing, after 7 days of *in vitro* culture and after 4 weeks of *in vivo* implantation. The hAFSC implants were incubated in osteogenic culture medium *in vitro* for 1 week and then implanted for 18 weeks, after which, bone tissue formation was observed. All the dSMCs showed similar mean potassium current and voltage values as non-printed control cell sample. After 8 weeks of implantation, the scaffolds with bECs showed abundantly and significantly more vascularization than scaffold-only implants. Thus, the authors showed the feasibility of inkjet bioprinting for *in vitro* fabrication of 3D heterogeneous tissues.

Apart from developing lab-on-a-chip devices, a big proportion of the 2D and 3D cell micropatterning research is focussed on tissue engineering and, therefore, some of its examples have been discussed in the next section.

8. Tissue engineering

8.1. Early research

Tissue engineering is one of the most important areas of application of inkjet bioprinting of mammalian cells. The multi-nozzle and layer-by-layer fabrication approach of inkjet bioprinting helps converge and assimilate multiple steps of tissue engineering into single broad step. As inkjet bioprinting is a drop-by-drop dispensing method, its application in tissue engineering has largely been limited to smaller scale tissue fabrication in comparison to other methods, such as extrusion bioprinting. However, it gains advantage in achieving a relatively higher, micron-scale printing resolution on tissue engineering substrates and scaffolds. For relatively simpler fabrication of small-sized structures resembling cartilage, bones, and straight tubular blood vessels, the use of conventional inkjet bioprinting with cell laden bioink is optimal, as has been shown in a number of previous researches. For example, Gao et al. [60] printed a bioink consisting of acrylated peptides, acrylated polyethylene glycol (PEGDMA), I-2959 photoinitiator, and bone marrow derived human mesenchymal stem cells (hMSCs) with simultaneous photopolymerization to form cell-laden hydrogel structures measuring 4 mm in diameter and 4 mm in height using a thermal inkjet printer. The cells showed even distribution throughout the hydrogel, 80–90% viability 24 h post-printing and, upon culture in chondrogenesis-specific and osteogenesis-specific media, proliferated and differentiated into cartilage-like and bone-like tissues through chondrogenesis and osteogenesis, respectively, as indicated by the increase in hydrogel compressive modulus, and secretion and deposition throughout the hydrogel of proteoglycans in chondrogenic differentiation and calcium in osteogenic differentiation. To fabricate blood vessel like tubular structures, Hewes et al. [61] used a piezoelectric inkjet printer with a single jetting device of 80 μm nozzle diameter. Human umbilical vein endothelial cells, HUVEC-turboGFP, were suspended in a mixture of alginate and fibrinogen and printed in a bath of calcium chloride and thrombin in the shape of a hollow cylinder. Free-standing tubular cell-laden hydrogel structures corresponding to blood microvessels and measuring 300 μm in diameter and 1–2 mm in height were, thus, obtained after just 2 min of printing for each structure. After 14 days of incubation in culture medium, majority of the cells were noted to have migrated towards the inner side of the scaffold and form a confluent monolayer similar to blood vessels, a process which shows similarities with angiogenesis.

8.2. Current research

While early research in tissue engineering remained limited to proof-of-concept studies and improving inkjet bioprinting technology by fabricating basic and small-scale cell-laden hydrogel structures, more sophisticated and tissue-specific inkjet bioprinting is being carried out in current research by adopting novel and more robust printing approach and developing hybrid inkjet bioprinting platforms. A novel approach of harnessing *in vivo* like cell-ECM interaction for cellular self-organization based tissue fabrication was shown by Park et al. [62] who patterned Detroit 551 and Hs68 human dermal fibroblasts with precisely controlled cell density on collagen hydrogel substrate through a piezo-electric inkjet printer. Post-printing cell-ECM interaction caused self-organization in the printed cells leading to formation of 3D cell-collagen microtissues. Also, precise and custom control over cell reorganization and 3D microtissue formation was achieved by controlled bioprinting with different cell densities, pattern size, and pattern shape, as confirmed by different sizes and shapes of the growing microtissues. The cells in the growing 3D microtissues showed elongated and stretched morphology with an even cell surface distribution of integrin α5β1, which is a marker for cell adhesion to ECM, and fibronectin, which is a marker for cell-cell and cell-ECM focal adhesions. Thus, the inkjet bioprinted microtissue was shown to be an accurate mimicry of *in vivo* tissues. Afterwards, a human skin model was constructed by inkjet bioprinting human epidermal keratinocytes on the patterned microtissue grown from Detroit 551 fibroblasts after 7-day culture. The bilayered skin model, thus produced, consisted of the upper epidermis and the lower papillary dermis microstructures at the dermo-epidermal junction. This research shows the potential of inkjet bioprinting to fabricate more complex and dynamic microenvironments of the human body. In an attempt to significantly increase the size of inkjet bioprinted tissue engineering scaffolds without increasing their fabrication time, Yoon et al. [64] developed an inkjet-spray printing method in which cell-laden bioink layers were printed with alternating fine spray of a cross-linking agent deposited by spray-coating technique as shown in Fig. 8 (a). To test their printing platform, NIH3T3 mouse fibroblasts and 293A human embryonic kidney cells were separately suspended in sodium alginate and printed with alternating spraying of calcium chloride to form hydrogels, as shown in Fig. 8 (b – c), with excellent post-printing viability of the embedded cells. This method allowed free-form, high-resolution and multi-layered printing of cell laden hydrogel structures, ranging at a large scale from <1 mm to >10 cm in size for the first time, and at relatively faster printing speeds of up to 75 mm/s which is much faster than in most previous studies. Afterwards, Hs68 human dermal fibroblasts, suspended in alginate-GelMA blend bioink, were printed to form hydrogel and cultured for 2 weeks during which the hydrogels maintained their shape and the cells showed normal cell spreading morphology and physiological functioning as confirmed by staining nuclei, f-actin, and collagen type I secreted by the fibroblasts. This novel technique holds the potential to be extended to multi-nozzle inkjet printers to build even larger scale hydrogel structures.

8.3. Different approaches

In another novel approach, Kim et al. [27] combined inkjet bioprinting with extrusion bioprinting to build a novel Integrated Composite tissue/organ Building System (ICBS). The ICBS possessed the capacity to separately and simultaneously dispense four and five biomaterials from its inkjet and extrusion modules, respectively, and consisted of a printing platform with high positional accuracy of 2.5 μm, 1 μm and 10 μm in x, y and z coordinates, respectively. To test its utility and efficacy, the authors built a human skin model with a functional
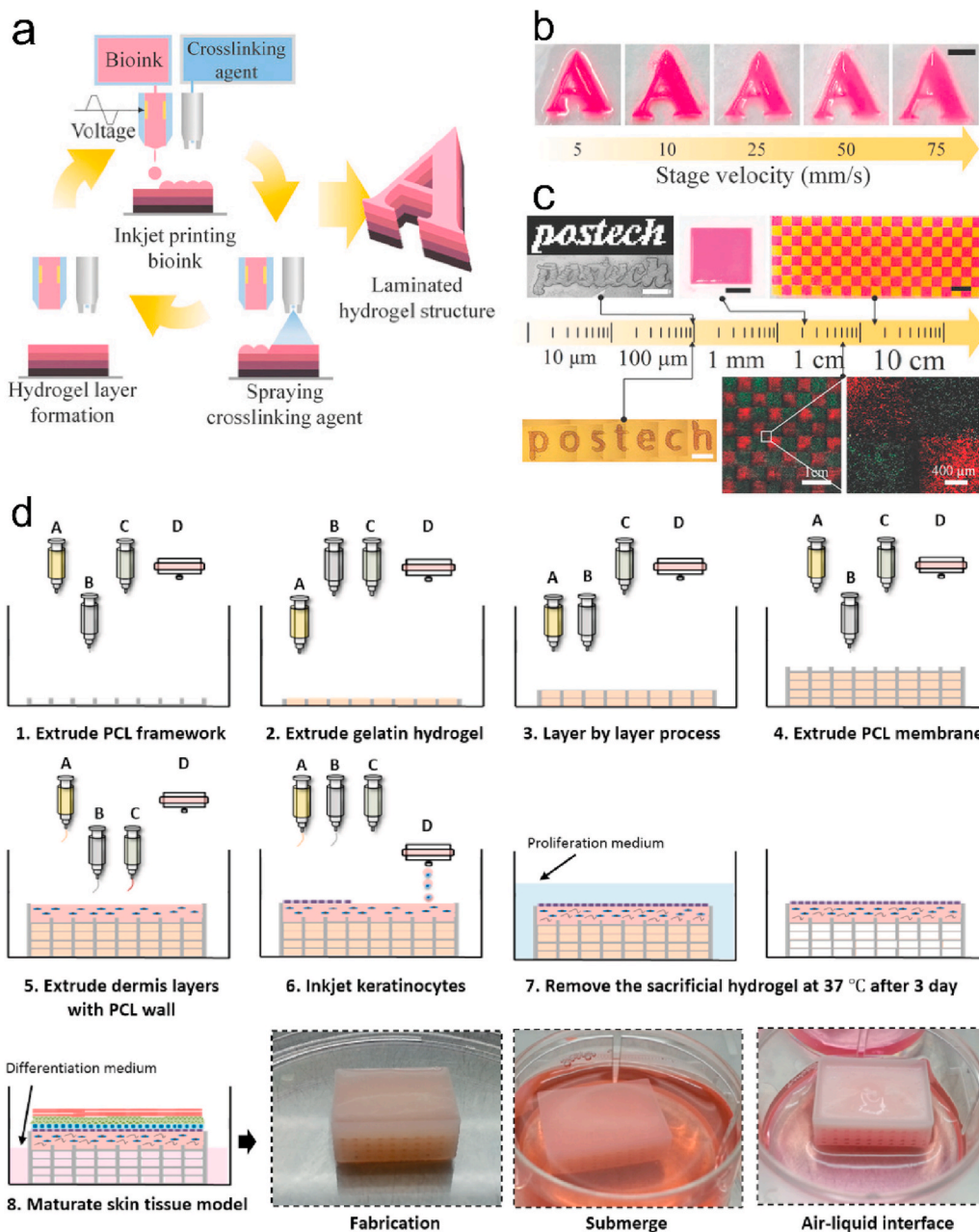
Fig. 8. (a) Schematic illustration of the inkjet printing – spray coating method for rapid fabrication of large cell-laden hydrogel scaffolds for applications in tissue engineering; **(b)** images of hydrogel letter-shape structures built at different printing speeds, showing minimal effect of speed and possibility of a rapid fabrication through inkjet bioprinting (scale bar: 5 mm); **(c)** images and light micrographs showing the range of scalability and high cell viability of the described method (scale bar: 1 cm in black, 1 mm in white unless otherwise mentioned). [image republished with permission from Ref. [64] Copyright © 2018 WILEY-VCH Verlag GmbH & Co. KGaA, Weinheim]. **(d)** Schematic illustration of the step-wise fabrication of human skin model with functional transwell system using a novel Integrated Composite tissue/organ Building System. **Nozzle A:** Sacrificial gelatin (extrusion); **Nozzle B:** supportive PCL (extrusion); **Nozzle C:** HDFs in collagen (extrusion); **Nozzle D:** HEKs in culture medium (inkjet). [image republished with permission from Ref. [27] Copyright © 2017 IOP Publishing Ltd].

transwell system in a broad single step as illustrated in Fig. 8 (d). The transwell system, which helps in culture, growth and maturation of the cells, is fabricated with a sacrificial gelatin bottom layer and polycaprolactone (PCL) as the supportive mesh for dermis using the extrusion module. Human primary dermal fibroblasts (HDFs) were suspended in collagen hydrogel and printed with the pneumatic extrusion printing module to form the dermis. Human primary epidermal keratinocytes (HEKs) were suspended in keratinocyte growth medium and printed with the piezoelectric inkjet printing module to form the epidermis. After 14 days of culture, a mature *in vitro* skin model with stretched dermis and stratified epidermis and a very high spatial resolution and uniform cell distribution is obtained alongside high cell viability and proliferation rates. Additionally, the keratinocytes showed a more widespread distribution of E-cadherin cell junction markers compared to the manually seeded control, representing that the printed cells in the skin model show tighter cell junctions and an enhanced and more

functional cell to cell interaction. It can, therefore, be said that the current trend in the application of inkjet bioprinting in tissue engineering is to actualize the *in vitro* inkjet bioprinting based fabrication of truly implantable tissues, such as skin, skeletal muscles, cardiac muscles, blood vessels, cartilage and bones, with favourable *in vivo* results.

As larger and larger 3D tissues are fabricated, diffusion limitations begin to pose an increasingly bigger challenge in successful exchange of gases, uptake of nutrients, removal of wastes, and thus, the long-term survival of cells. In an attempt to solve the perfusion limitation problem in 3D tissue models, Negro et al. [63] printed a mixture of sodium alginate and PEG with crosslinkable active transglutaminase factor XIII to resemble the extracellular matrix (ECM), and simultaneously printed C2C12 muscle progenitor cells, suspended in sacrificial sodium alginate, inside the ECM layers using a piezoelectric inkjet printing based commercial Microdrop Autodrop system. On selective digestion of alginate with alginate lyase enzyme in pre-determined 3D pattern, microfluidic

or perfusion networks resembling simple *in vivo* vascular networks were formed. The cells left in the space after the removal of sacrificial alginate showed normal proliferation while leaving enough space for easy perfusion of culture medium and gases. Afterwards, the authors also printed NIH 3T3 fibroblasts suspended in sodium alginate to show formation of hydrogel structures in various shapes, with high precision of 100 μm, with large size range of up to several centimetres, and with high cell viability of >90% at 4 h post-printing. This work, thus, shows a high potential of inkjet bioprinting to solve one of the key challenges of *in vitro* tissue engineering and organ fabrication which is the inability of the current bioprinting techniques to integrate an intricate network of vasculature throughout the volume of the *in vitro* fabricated 3D tissues [95].

9. *In vivo* cell printing

9.1. Current research

When inkjet bioprinting is used to deposit cells directly at a desired site, such as a wound, in a living organism, the procedure is called *in vivo* cell printing and it holds substantial potential for improving the treatment of large burns, chronic wounds, and even deep tissue injuries. Fast and aseptic healing of acute or chronic skin wounds is essential to prevent further infections or hypertrophic scarring. It is especially important if the wound has a large surface area and/or is deep such as those in the case of ulcers, burns and diabetic wounds. In such wounds, the conventional treatment strategies using bandages and ointments often

fail or result in delayed healing. The application of natural or artificial skin grafts provide relatively better results, but such a clinical practice is often limited by the unavailability of such grafts or allergy and graft rejection [112]. For sorting out such limitations, Albanna et al. [65] applied the inkjet bioprinting technique to directly print living skin cells on skin wounds, as illustrated in Fig. 9 (a – d), and assess the wound healing capability. Skin wounds were created by surgical excision and removal of a small part of dorsal skin in murine and porcine models. A handheld laser scanner was then used to scan the wounds for creating their 3D maps to be converted to CAD for cell printing. For printing on the murine model, human cells were used as a proof-of-concept study to show the capability of inkjet bioprinting of constructing a human skin mimic and the printability of human skin cells and their post-printing potency of forming a functional skin. Human dermal fibroblasts and epidermal keratinocytes, both suspended in a mixture of fibrinogen and collagen, were filled in two separate cartridges and a third cartridge was filled with thrombin. First, the fibroblasts were printed on the wound, followed by printing of thrombin to cross-link the fibrinogen and form a stable matrix. After allowing cross-linking for 15 min, the keratinocytes were printed, again followed by printing of thrombin. The wounds showed epithelium formation by week 1 and complete wound closure by week 3. In comparison, the untreated wounds and wounds printed with cell-less fibrinogen-collagen-thrombin matrix showed open wound areas up to week 4 due to slow and poor epithelialization. Immunohistochemistry assay with anti-human nuclear antigen showed the post-printing presence of human fibroblasts and keratinocytes in the healing wounds up to week 3 and week 6, respectively. For the porcine
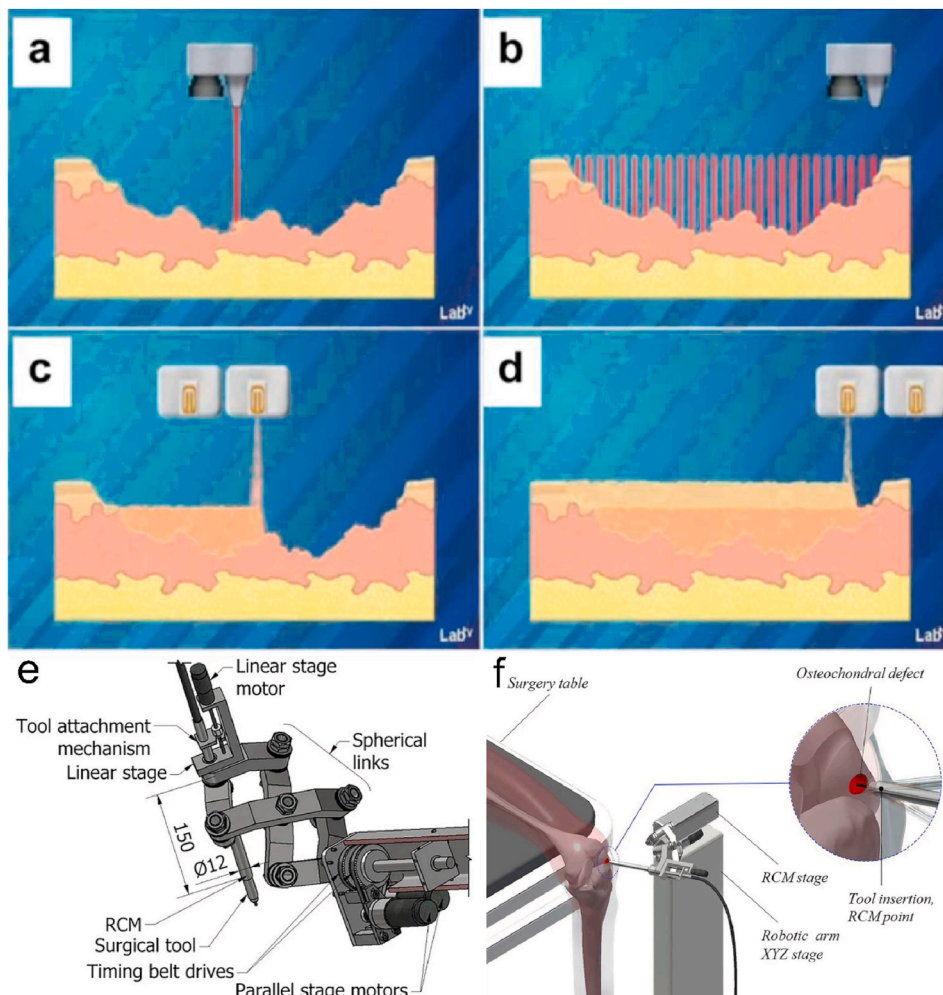

Fig. 9. Schematic illustration of *in vivo* inkjet printing of skin cells on an open wound for faster and scar-free healing. **(a)** A laser scans the contour of the wound in 3D; **(b)** the computer makes a 3D map of the volume to be printed and calculates the specific amount and type of the cells to be printed on the different sites of the wound; **(c)** the inner dermal cells are printed first; **(d)** the outer epidermal cells are printed on top of the dermal layer. [images a – d republished with permission from Ref. [65] Copyright © 2019 Springer Nature]. **(e)** Schematic illustration of the design of a robotic arm with remote centre of motion (RCM) which confers six degrees of freedom (x, y, z, yaw, pitch and roll). The end of the arm can be fitted with an inkjet printing device as per the need. **(f)** Schematic illustration of a proposed set-up in which surgery and cell printing is being conducted *in vivo* on a diseased or wounded knee joint. [images e – f republished with permission from Ref. [67] Copyright © 2019 Springer Nature].

models, allogeneic and autologous cells were used, with the same printing procedure, as autologous and allogeneic testing done on porcine models better mimic the human skin healing in comparison to the murine model which has different skin healing rates and mechanisms. The wounds printed with autologous fibroblasts and keratinocytes showed faster closure, lesser contraction at the edges, higher re-epithelialization, and much intense network of blood vessels throughout epidermis and dermis by week 4 to week 8, thus, resulting in least scarring in comparison to the wounds printed with allogeneic cells, cell-less matrix and untreated wounds. On comparing the results to the manual cell spraying technique which is applied in current clinical practice, this bioprinting technique provided similar results. On the other hand, one advantage of this technique was that the cells could be deposited separately in an accurate and custom layer-by-layer pattern rather than depositing an unorganized mixture of both cell types which leads to failures or sub-optimal results as in the manual method.

9.2. Integration of robotics

All the previously mentioned inkjet printing technologies possess two (X, Y) or three (X, Y, Z) degrees of freedom while printing. In addition to forward-backward (X), left-right (Y) and up-down (Z) movements, a conventional robotic arm with remote centre of motion (RCM), as illustrated in Fig. 9 (e), can perform roll, pitch and yaw forms of movement. Printing with an inkjet bioink dispenser attached at the end of a robotic arm, however, can provide six degrees of freedom instead of the conventional maximum of the three Cartesian directions of movement [67]. Such a technique can enable cell printing in 3D space for fabricating complex *in vivo* mimics with precise cell/tissue localization, and in those medical cases which require direct cell application therapies, such as printing *in vivo* directly at the site of injury for faster healing of musculoskeletal injuries, chronic wounds and burnt skin. Robotic arm-based 3D bioprinting, thus, has a high potential of solving the current challenges of healing critical tissue defects and developing minimally invasive surgery procedures as illustrated in Fig. 9 (f). Inkjet bioprinting can, thus, not only print the 2D patterns of cells in several layers to form a 3D tissue *in vivo*, but it will also have the capability to move around in 3D space with no restriction in the choice of printing location. Furthermore, with all the bioprinting technologies, *in vitro* biofabrication of vascularized soft organs, purposed for organ transplantation, remains a challenge [19]. As described earlier, inkjet bioprinting can print one cell at time in any desired pattern. Combining it with the robotic six degrees of freedom of movement and the inherent capacity of cells to differentiate, organize and exhibit controlled growth, as seen during developmental morphogenesis [66], holds the potential, at least in theory, to revolutionize *in vitro* tissue and organ fabrication.

9.3. Multi-purpose applications

An advanced application of *in vivo* cell printing, by combining it with gene transfection of the printing cells, was investigated by Xu et al. [40] by direct inkjet co-printing of porcine aortic endothelial (PAE) cells mixed with pmaxGFP plasmids into the subcutaneous tissues of athymic or nude mice. Before printing cells, fibrinogen and thrombin were printed in alternate layers *in vivo* into the subcutaneous tissue in order to form an implanted cuboid fibrin structure or scaffold, that could allow easy retrieval of cells later for analysis. After cell printing on it, the structure was left implanted for 7 days after which it was surgically removed, washed and analysed. The structure was found to retain its initial cuboid shape and the printed cells embedded in the fibrin structure showed high viability along with GFP expression, indicating successful gene transfection. Conducting such simultaneous procedures may help in the future in medical cases requiring cell transplantation, where any genetic or metabolic defect in the cells is corrected through appropriate gene transfection and the transfected cells are printed at the required location *in vivo*.

10. Conclusion, challenges and future prospects

In this detailed review, we have seen the versatility of piezoelectric and thermal inkjet printing of mammalian cells by means of its widespread and evolving applications in intracellular delivery and transfection, gene expression modification, single cell sorting, cell microarray, cell micropatterning, tissue engineering and *in vivo* printing. This has become possible because of the pliability of inkjet bioprinting technology in dispensing various cell formulations and in fabricating cell-laden structures in various shapes and sizes, from the simple dots, straight lines and circles to complex 2D and 3D geometries.

While some areas of application, such as cell microarray, have seen the emergence of commercial inkjet cell printers, the others are not yet in a state of being taken out of the laboratory and into the commercial biomedical market. Some of the reasons behind this limitation include the lack of a universal printer form factor, the development of a large number of different protocols for bioink formulation, and the requirement of different cell and biomaterial types in different cases. Apart from this, different areas of application of inkjet cell printing have different magnitudes of strengths and weaknesses. In gene transfection and gene expression modification, for example, inkjet cell printing is currently not in a position to compete against the well-established laboratory techniques, such as electroporation for gene transfection, and genetic engineering for gene expression modification. For tissue engineering, even though its high resolution is unmatched, inkjet cell printing would need continuous innovation in order to significantly increase the volume of cell and scaffold samples that can be printed in a given amount of time. Low printing volume is also a limiting factor in case of *in vivo* cell printing.

On analysing the current research, it can be deduced that two main trends are ongoing. First is the continuous optimization of printing parameters, such as voltage; evolution of the printing equipment, such as imaging for single cell sorting; and adjustment of bioink formulations, such as cell density, in an attempt to make inkjet cell printing more accurate, advanced and relevant to the specific requirements. Such ongoing studies will help eliminate the current disadvantages, such as lack of commercial scalability which is posing as a roadblock to a much wider acceptance of the inkjet bioprinting technology. Second is the printing of cells with higher *in vitro* structural volume and an even higher-than-before resolution, better controllability over printed cell physiology and accurate batch to batch reproducibility. This will help replace lesser efficient laboratory techniques, such as conventional biomedical assays, and generate *in vitro* co-cultures and large 3D models of several cells to mimic the *in vivo* systems more accurately when compared against the conventional flask or plate based 2D cell cultures. Several research groups and companies have, over the years, developed different types of inkjet cell printing tools and methodologies which would require a convergent evolution in the future along with the establishment of broad universal principles which would dictate the application of inkjet cell printing in different cases and with minimal drawbacks.

Declaration of competing interest

The authors declare that there is no conflict of interest.

Acknowledgements

References

[1] J. Alaman, R. Alicante, J.I. Pena, C. Sanchez-Somolinos, Materials 9 (2016) 910.
[2] C. Mandrycky, Z. Wang, K. Kim, D.H. Kim, Biotechnol. Adv. 34 (2016) 422.
[3] S.V. Murphy, A. Atala, Nat. Biotechnol. 32 (2014) 773.
[4] P. Calvert, Science 318 (2007) 208.

[5] J. Li, F. Rossignol, J. Macdonald, Lab Chip 15 (2015) 2538.
[6] L. Gonzalez-Macia, A.J. Killard, Woodh Publ Ser Biom 118 (2017) 69.
[7] T.G. Henares, K. Yamada, K. Suzuki, D. Citterio, in: Design of Polymeric Platforms for Selective Biorecognition, Eds., Springer, 2015, p. 197.
[8] B. Derby, Annu. Rev. Mater. Res. 40 (2010) 395.
[9] R.E. Saunders, B. Derby, Int. Mater. Rev. 59 (2014) 430.
[10] K. Holzl, S.M. Lin, L. Tytgat, S. Van Vlierberghe, L.X. Gu, A. Ovsianikov, Biofabrication 8 (2016).
[11] P.M. Grubb, H. Subbaraman, S. Park, D. Akinwande, R.T. Chen, Sci. Rep. 7 (2017) 1202.
[12] N. Karim, S. Afroj, S.R. Tan, K.S. Novoselov, S.G. Yeates, Sci Rep-Uk 9 (2019) 8035.
[13] F. Molina-Lopez, T.Z. Gao, U. Kraft, C. Zhu, T. Ohlund, R. Pfattner, V.R. Feig, Y. Kim, S. Wang, Y. Yun, Z. Bao, Nat. Commun. 10 (2019) 2676.
[14] X. Cui, T. Boland, D.D. D'Lima, M.K. Lotz, Recent Pat. Drug Deliv. Formulation 6 (2012) 149.
[15] J. Goole, K. Amighi, Int. J. Pharm. 499 (2016) 376.
[16] L.K. Prasad, H. Smyth, Drug Dev. Ind. Pharm. 42 (2016) 1019.
[17] T. Moroni, T. Boland, J.A. Burdick, C. De Maria, B. Derby, G. Forgacs, J. Groll, Q. Li, J. Malda, V.A. Mironov, C. Mota, M. Nakamura, W. Shu, S. Takeuchi, T.B. F. Woodfield, T. Xu, J.J. Yoo, G. Vozzi, Trends Biotechnol. 36 (2018) 384.
[18] J. Groll, J.A. Burdick, D.W. Cho, B. Derby, M. Gelinsky, S.C. Heilshorn, T. Jüngst, J. Malda, V.A. Mironov, K. Nakayama, A. Ovsianikov, W. Sun, S. Takeuchi, J. J. Yoo, T.B.F. Woodfield, Biofabrication 11 (2018), 013001.
[19] V. Mironov, T. Boland, T. Trusk, G. Forgacs, R.R. Markwald, Trends Biotechnol. 21 (2003) 157.
[20] W.C. Wilson Jr., T. Boland, The anatomical record, Part A, Discoveries in molecular, cellular, and evolutionary biology 272 (2003) 491.
[21] T. Boland, V. Mironov, A. Gutowska, E.A. Roth, R.R. Markwald, Anat. Rec. Part A 272A (2003) 497.
[22] S. Barui, R.E. Saunders, S. Naskar, B. Basu, B. Derby, ACS Biomater. Sci. Eng. 6 (2020) 749.
[23] C. Tse, R. Whiteley, T. Yu, J. Stringer, S. MacNeil, J.W. Haycock, P.J. Smith, Biofabrication 8 (2016), 015017.
[24] M. Nakamura, A. Kobayashi, F. Takagi, A. Watanabe, Y. Hiruma, K. Ohuchi, Y. Iwasaki, M. Horie, I. Morita, S. Takatani, Tissue Eng. 11 (2005) 1658.
[25] N. Antill-O'Brien, J. Bourke, C.D. O'Connell, Materials 12 (2019) 3218.
[26] R. Wenger, M. Mauron, F. Bircher, R. Nussbaumer, in: TERMIS European Chapter Meeting 2019, 2019. Rhodes, Greece.
[27] B.S. Kim, J.S. Lee, G. Gao, D.W. Cho, Biofabrication 9 (2017), 025034.
[28] A. Yusof, H. Keegan, C.D. Spillane, O.M. Sheils, C.M. Martin, J.J. O'Leary, R. Zengerle, P. Koltay, Lab Chip 11 (2011) 2447.
[29] A.R. Liberski, J.T. Delaney Jr., U.S. Schubert, ACS Comb. Sci. 13 (2011) 190.
[30] J.A. Park, S. Yoon, J. Kwon, H. Now, Y.K. Kim, W.J. Kim, J.Y. Yoo, S. Jung, Sci. Rep. 7 (2017) 14610.
[31] X.D. Li, J.W. Chen, B.X. Liu, X. Wang, D.N. Ren, T. Xu, Ref Ser Biomed Eng (2018) 283.
[32] A. Folch, M. Toner, Annu. Rev. Biomed. Eng. 2 (2000) 227.
[33] A. Azioune, M. Storch, M. Bornens, M. Thery, M. Piel, Lab Chip 9 (2009) 1640.
[34] J. Ziauddin, D.M. Sabatini, Nature 411 (2001) 107.
[35] W. Xu, A.M. Luikart, C.E. Sims, N.L. Allbritton, Anal. Bioanal. Chem. 397 (2010) 3377.
[36] J.R. Rettig, A. Folch, Anal. Chem. 77 (2005) 5628.
[37] Y. Tokimitsu, H. Kishi, S. Kondo, R. Honda, K. Tajiri, K. Motoki, T. Ozawa, S. Kadowaki, T. Obata, S. Fujiki, C. Tateno, H. Takaishi, K. Chayama, K. Yoshizato, E. Tamiya, T. Sugiyama, A. Muraguchi, Cytometry Part A : the journal of the International Society for Analytical Cytology 71 (2007) 1003.
[38] A. Rosenthal, A. Macdonald, J. Voldman, Biomaterials 28 (2007) 3208.
[39] S. Iwanaga, K. Arai, M. Nakamura, in: A. Atala, J.J. Yoo (Eds.), Essentials of 3D Biofabrication and Translation, Eds., Academic Press, Boston, 2015, p. 61.
[40] T. Xu, J. Rohozinski, W.X. Zhao, E.C. Moorefield, A. Atala, J.J. Yoo, Tissue Eng. 15 (2009) 95.
[41] A.B. Owczarczak, S.O. Shuford, S.T. Wood, S. Deitch, D. Dean, Jove-J Vis Exp 61 (2012), e3681.
[42] X. Cui, D. Dean, Z.M. Ruggeri, T. Boland, Biotechnol. Bioeng. 106 (2010) 963.
[43] L.H. Solis, Y. Ayala, S. Portillo, A. Varela-Ramirez, R. Aguilera, T. Boland, Biofabrication 11 (2019), 045005.
[44] A. Campbell, A. Philipovskiy, R. Heydarian, A. Varela-Ramirez, D.A. Gutierrez, L. H. Solis, M.E. Furth, T. Boland, J. Clin. Oncol. 37 (2019) S2605.
[45] A. Campbell, J.E. Mohl, D.A. Gutierrez, A. Varela-Ramirez, T. Boland, Frontiers in bioengineering and biotechnology 8 (2020) 82.
[46] M. Yumoto, N. Hemmi, N. Sato, Y. Kawashima, K. Arikawa, K. Ide, M. Hosokawa, M. Seo, H. Takeyama, Sci Rep-Uk 10 (2020) 7158.
[47] T. Xu, H. Kincaid, A. Atala, J.J. Yoo, J Manuf Sci E-T Asme 130 (2008), 021017.
[48] A. Gross, J. Schondube, S. Niekrawitz, W. Streule, L. Riegger, R. Zengerle, P. Koltay, J. Lab. Autom. 18 (2013) 504.
[49] R. The, S. Yamaguchi, A. Ueno, Y. Akiyama, K. Morishima, Ieee Int C Int Robot (2013) 502.
[50] F. Stumpf, J. Schoendube, A. Gross, C. Rath, S. Niekrawietz, R. Koltay, G. Roth, Biosens. Bioelectron. 69 (2015) 301.
[51] W.H. Yoon, H.R. Lee, S. Kim, E. Kim, J.H. Ku, K. Shin, S. Jung, Biofabrication 12 (2020), 035030.
[52] R. Jonczyk, S. Timur, T. Scheper, F. Stahl, J. Biotechnol. 217 (2016) 109.
[53] T.M. Park, D. Kang, I. Jang, W.S. Yun, J.H. Shim, Y.H. Jeong, J.Y. Kwak, S. Yoon, S. Jin, Int. J. Mol. Sci. 18 (2017) 2348.
[54] S. Mi, S. Yang, T. Liu, Z. Du, Y. Xu, B. Li, W. Sun, IEEE Trans. Biomed. Eng. 66 (2019) 2512.
[55] T. Xu, J. Jin, C. Gregory, J.J. Hickman, T. Boland, Biomaterials 26 (2005) 93.
[56] T. Xu, C.A. Gregory, P. Molnar, X. Cui, S. Jalota, S.B. Bhaduri, T. Boland, Biomaterials 27 (2006) 3580.
[57] M. Matsusaki, K. Sakaue, K. Kadowaki, M. Akashi, Adv Healthc Mater 2 (2013) 534.
[58] X.F. Cui, T. Boland, Biomaterials 30 (2009) 6221.
[59] T. Xu, W.X. Zhao, J.M. Zhu, M.Z. Albanna, J.J. Yoo, A. Atala, Biomaterials 34 (2013) 130.
[60] G. Gao, T. Yonezawa, K. Hubbell, G. Dai, X. Cui, Biotechnol. J. 10 (2015) 1568.
[61] S. Hewes, A.D. Wong, P.C. Searson, Bioprinting 7 (2017) 14.
[62] J.A. Park, H.R. Lee, S.Y. Park, S. Jung, Advanced biosystems 4 (2020), e1900280.
[63] A. Negro, T. Cherbuin, M.P. Lutolf, Sci. Rep. 8 (2018) 17099.
[64] S. Yoon, J.A. Park, H.R. Lee, W.H. Yoon, D.S. Hwang, S. Jung, Adv Healthc Mater 7 (2018), e1800050.
[65] M. Albanna, K.W. Binder, S.V. Murphy, J. Kim, S.A. Qasem, W. Zhao, J. Tan, I. B. El-Amin, D.D. Dice, J. Marco, J. Green, T. Xu, A. Skardal, J.H. Holmes, J. D. Jackson, A. Atala, J.J. Yoo, Sci. Rep. 9 (2019) 1856.
[66] V. Mironov, G. Prestwich, G. Forgacs, J. Mater. Chem. 17 (2007) 2054.
[67] J. Lipskas, K. Deep, W. Yao, Sci Rep-Uk 9 (2019) 3746.
[68] S. Sohrabi, Y.L. Liu, Phys. Rev. E 97 (2018), 033105.
[69] S. Chen, G.D. Doolen, Annu. Rev. Fluid Mech. 30 (1998) 329.
[70] L. Chen, Q.J. Kang, Y.T. Mu, Y.L. He, W.Q. Tao, Int. J. Heat Mass Tran. 76 (2014) 210.
[71] D.A. Fedosov, B. Caswell, G.E. Karniadakis, in: Conference Proceedings : ... Annual International Conference of the IEEE Engineering in Medicine and Biology Society. IEEE Engineering in Medicine and Biology Society. Annual Conference 2009, 2009, p. 4266.
[72] S. Sohrabi, Y.L. Liu, Artif. Organs 41 (2017) E80.
[73] D.A. Fedosov, J. Fornleitner, G. Gompper, Phys. Rev. Lett. 108 (2012), 028104.
[74] Y. Ujihara, M. Nakamura, H. Miyazaki, S. Wada, Ann. Biomed. Eng. 38 (2010) 1530.
[75] D.A. Fedosov, B. Caswell, G.E. Karniadakis, Biophys. J. 98 (2010) 2215.
[76] K. Koshiyama, S. Wada, J. Biomech. 44 (2011) 2053.
[77] B. Lorber, W.K. Hsiao, I.M. Hutchings, K.R. Martin, Biofabrication 6 (2014), 015001.
[78] R. Detsch, S. Blob, T. Zehnder, R. Boccaccini Aldo, BioNanoMaterials 17 (2016) 185.
[79] F. Salaris, A. Rosa, Brain Res. 1723 (2019), 146393.
[80] I. Kelava, M.A. Lancaster, Dev. Biol. 420 (2016) 199.
[81] R.E. Saunders, J.E. Gough, B. Derby, Biomaterials 29 (2008) 193.
[82] E. Cheng, H. Yu, A. Ahmadi, K.C. Cheung, Biofabrication 8 (2016), 015008.
[83] M.Y. Zhang, S. Krishnamoorthy, H.T. Song, Z.Y. Zhang, C.X. Xu, J. Appl. Phys. 121 (2017), 124904.
[84] J. Gehl, Acta Physiol. Scand. 177 (2003) 437.
[85] Nat. Methods 3 (2006) 67.
[86] C.E. Thomas, A. Ehrhardt, M.A. Kay, Nat. Rev. Genet. 4 (2003) 346.
[87] M. Finer, J. Glorioso, Gene Ther. 24 (2017) 1.
[88] P.L. Felgner, T.R. Gadek, M. Holm, R. Roman, H.W. Chan, M. Wenz, J. P. Northrop, G.M. Ringold, M. Danielsen, Proc. Natl. Acad. Sci. U. S. A. 84 (1987) 7413.
[89] E. Dodds, M.G. Dunckley, K. Naujoks, U. Michaelis, G. Dickson, Gene Ther. 5 (1998) 542.
[90] F. Cardarelli, L. Digiacomo, C. Marchini, A. Amici, F. Salomone, G. Fiume, A. Rossetta, E. Gratton, D. Pozzi, G. Caracciolo, Sci. Rep. 6 (2016) 25879.
[91] A. Hamm, N. Krott, I. Breibach, R. Blindt, A.K. Bosserhoff, Tissue Eng. 8 (2002) 235.
[92] S.M. Byrne, P. Mali, G.M. Church, in: J.A. Doudna, E.J. Sontheimer (Eds.), Methods in Enzymology, Eds., Academic Press, 2014, p. 119.
[93] C.A. Clement, L.A. Larsen, S.T. Christensen, in: R.D. Sloboda (Ed.), Methods in Cell Biology, Eds., Academic Press, 2009, p. 181.
[94] S.Y. Hann, H. Cui, T. Esworthy, S. Miao, X. Zhou, S.J. Lee, J.P. Fisher, L.G. Zhang, Transl. Res. : J. Lab. Clin. Med. 211 (2019) 46.
[95] S.V. Murphy, P. De Coppi, A. Atala, Nature biomedical engineering 4 (2020) 370.
[96] M.E. Murphy, Carcinogenesis 34 (2013) 1181.
[97] D. Mahalingam, R. Swords, J.S. Carew, S.T. Nawrocki, K. Bhalla, F.J. Giles, Br. J. Canc. 100 (2009) 1523.
[98] O.N. Mikhailova, L.F. Gulyaeva, M.L. Filipenko, Toxicology 210 (2005) 189.
[99] A. Cossarizza, H.-D. Chang, A. Radbruch, M. Akdis, I. Andrä, F. Annunziato, et al., Eur. J. Immunol. 47 (2017) 1584.
[100] B. Rosental, Z. Kozhekbaeva, N. Fernhoff, J.M. Tsai, N. Traylor-Knowles, BMC Cell Biol. 18 (2017) 30.
[101] P. Hu, W. Zhang, H. Xin, G. Deng, Front Cell Dev Biol 4 (2016) 116.
[102] S.J. Tan, M.Z. Kee, A.S. Mathuru, W.F. Burkholder, S.J. Jesuthasan, PloS One 8 (2013), e78261.
[103] P.H. Burkill, C.P. Gallienne, in: J.H. Steele (Ed.), Encyclopedia of Ocean Sciences, second ed., Academic Press, Oxford, 2001, p. 243.
[104] H.J. Hong, W.S. Koom, W.G. Koh, Sensors 17 (2017) 1293.
[105] O.I. Berthuy, S.K. Muldur, F. Rossi, P. Colpo, L.J. Blum, C.A. Marquette, Lab Chip 16 (2016) 4248.
[106] R. Jonczyk, T. Kurth, A. Lavrentieva, J.G. Walter, T. Scheper, F. Stahl, Microarrays 5 (2016) 11.
[107] M.L. Yarmush, K.R. King, Annu. Rev. Biomed. Eng. 11 (2009) 235.
[108] A. Martinez-Rivas, G.K. Gonzalez-Quijano, S. Proa-Coronado, C. Severac, E. Dague, Micromachines 8 (2017) 347.

[109] M. Thery, A. Jimenez-Dalmaroni, V. Racine, M. Bornens, F. Julicher, Nature 447 (2007) 493.

[110] G. Letort, A.Z. Politi, H. Ennomani, M. Thery, F. Nedelec, L. Blanchoin, PLoS Comput. Biol. 11 (2015), e1004245.

[111] R.J. Klebe, Exp. Cell Res. 179 (1988) 362.

[112] S. Dixit, D.R. Baganizi, R. Sahu, E. Dosunmu, A. Chaudhari, K. Vig, S.R. Pillai, S. R. Singh, V.A. Dennis, J. Biol. Eng. 11 (2017) 49.